Biochimica et Biophysica Acta 1827 (2013) 1258–1277

Contents lists available at ScienceDirect

Biochimica et Biophysica Acta

journal homepage: www.elsevier.com/locate/bbabio

Review

Unanswered questions about the structure of cytochrome bc_1 complexes ☆

Edward A. Berry *, Heather De Bari [1], Li-Shar Huang

Department of Biochemistry and Molecular Biology, SUNY Upstate Medical University, Syracuse, NY 13210, USA

ARTICLE INFO

Article history:
Received 13 December 2012
Received in revised form 13 March 2013
Accepted 16 April 2013
Available online 25 April 2013

Keywords:
Ubiquinol:cytochrome c reductase
Complex III
Heme protein
Heme orientation
Non-pro cis peptide
Rieske iron-sulfur protein
Matrix processing peptidase

ABSTRACT

X-ray crystal structures of bc1 complexes obtained over the last 15 years have provided a firm structural basis for our understanding of the complex. For the most part there is good agreement between structures from different species, different crystal forms, and with different inhibitors bound. In this review we focus on some of the remaining unexplained differences, either between the structures themselves or the interpretations of the structural observations. These include the structural basis for the motion of the Rieske iron–sulfur protein in response to inhibitors, a possible conformational change involving tyrosine132 of cytochrome (cyt) b, the presence of *cis*-peptides at the beginnings of transmembrane helices C, E, and H, the structural insight into the function of the so-called "Core proteins", different modelings of the retained signal peptide, orientation of the low-potential heme *b*, and chirality of the Met ligand to heme c_1. This article is part of a Special Issue entitled: Respiratory complex III and related bc complexes.

1. Introduction

In the last two decades crystal structures have become available for bc_1 complexes from vertebrates, yeast, and α-proteobacteria; and b_6f complexes from chloroplasts and cyanobacteria. What have they told us? Reassuringly, they did not reveal any features incompatible with the "modified Q-cycle" mechanism for coupling proton pumping to electron transfer, which had been pretty well adopted by the time of the first structures. Two inhibitor-binding sites were identified corresponding to the Q_N and Q_P sites located on opposite sides of the membrane near the b_H and b_L hemes respectively. The b hemes provide a path for electrons between the sites, as inferred from the "double kill" experiments [1,2] and required by the Q cycle mechanism. The structures mainly confirmed the picture that had been built up from years of theorizing, biophysical experimentation, site-directed and inhibitor-resistant mutagenesis, and bioinformatics [3,4]. One surprise was the requirement for movement of the Rieske iron–sulfur protein (ISP) for electron transport from the Q_P site to cyt c_1, opening up new possibilities for gating to enforce the bifurcated reaction. Another stimulating result is the fact that the heme b_L moieties in the two monomers are within effective electron transfer distance on a kinetically competent time scale, leading to questions about the importance of inter-monomer electron transfer. Both *b* hemes are close to their respective membrane surfaces, consistent with reactivity with water soluble reagents [5] but leaving unexplained the apparently large electrogenic step for electron transfer between heme b_H and quinone at the Q_N site. Perhaps the biggest disappointment is that no reliable structure for quinone or quinol at the Q_P site has been obtained. Thus the structures have not contributed as much as might be expected to explaining the mechanism of the bifurcated reaction. But it seems reasonable to assume that quinone binds (for at least part of the reaction) in the position of stigmatellin or nHDBT, with an H-bond to a ligand of the Fe_2S_2 cluster. By providing accurate position of the redox centers including the ISP cluster in multiple positions, the structures provide distances between redox centers. These, together with extensive kinetic data mainly from flash-activated experiments in the photosynthetic systems, strongly constrain the type of mechanisms that can be considered [6].

Crystal structures of the bc_1 complex have been obtained from seven crystal forms of the mitochondrial complex, from beef, chicken, and yeast; and four forms of the bacterial complex, from two species of *Rhodobacter* and *Paracoccus denitrificans*. Cytochrome b_6f structures are available from two additional crystal forms. Table 1 lists the different

Abbreviations[2]: Q_P, Q_N, quinone processing active sites of the bc complex near the negative (−) and positive (Q_P) surfaces of the energy transducing membrane; cyt, cytochrome; ISP, iron–sulfur protein; nHDBT, alkylhydroxydioxobenzothiazole; MPP, matrix processing peptidase of mitochondria; MIP, matrix intermediate peptidase; IC_{50}, inhibitor concentration giving 50% inhibition; NCS, noncrystallographic symmetry; ASU, asymmetric unit; PDB, protein databank; E_m, pH dependent standard reduction potential E′°.

☆ This article is part of a Special Issue entitled: Respiratory complex III and related bc complexes.

* Corresponding author. Tel.: +1 315 464 8751.
E-mail address: BerryE@upstate.edu (E.A. Berry).
[1] Current address: National Heart, Lung, and Blood Institute, 31 Center Drive MSC 2486, Bethesda, MD 20892, USA.

[2] Structures deposited in the pdb are referred to by their 4-character ID codes, lower or upper case as least ambiguous. Amino acids are referred to with their standard 3-letter or one-letter codes, followed by sequence number if appropriate. The two crystal forms that are the main subject, the tetragonal ($I4_122$) crystals of bovine bc_1 and the orthorhombic ($P2_12_12_1$) crystals of chicken bc_1 are referred to as the tetragonal crystals and chicken crystals, respectively.

0005-2728/$ – see front matter © 2013 Elsevier B.V. All rights reserved.
http://dx.doi.org/10.1016/j.bbabio.2013.04.006

Table 1
Different crystal forms of the cytochrome bc_1 and b_6f complexes that have provided structures.

Source	Space group	Ref.	Examples	bc_1/AU	Best resolution	ISP-ED[a] b, c_1, or mobile	Data available?	SU11/ QCR10; SU4?
Beef								
	$I4_122$	[7]	1qcr, 2fyu	1	2.3	m	N	Y
	$P6_522$	[8,9]	1be3	1	3.0	c_1	N	Y
	$P6_5$	[9]	1bgy	2	3.0 (2.5[b])	I, m	N	Y
	$P2_12_12_1$	[10]	1ppj, 2a06	2	2.1	b, b	Y	N
Chicken								
	$P2_12_12_1$	[8]	1bcc, 3h1h, 3L70	2	2.7	m, m	Y	N
Yeast								
	C2	[11]	1ezv, 1kb9, 1p84	1	2.3	b	N	N
	$P2_1$	[12,13]	1kyo, 3cx5	2	1.9	b,b	Y	N
Rb. caps.								
	$P2_1$	[14]	1zrt	2	3.5	b	Y	na
Rb. sph.								
	C2	[15,16]	2fyn, 2qJk, 2qJy	6	2.4	b	Y	N
	$P2_1$	[16]	2qJp	4	2.6	b	Y	N
Pc. deni.								
	$P2_1$	[17]	2yiu	2	2.7		Y	na
Chlamy.								
	I222	[18]	1q90	1	3.1		Y	
Mastigo., Nostoc	$P6_122$	[19]	2e74, 2zt9	1	3.0		Y	

[a] Position or state of the ISP extrinsic domain. "Mobile" implies the ability to move in the crystal, although it may be fixed in **b** or **c1** position in particular structures, especially in the presence of inhibitors. "I" refers to an intermediate position seen in one monomer of structure 1bgy.
[b] Resolution in parentheses is unpublished but reported at meetings or otherwise known.

crystal forms and some of their characteristics. Having multiple crystal forms has been very beneficial, as the different forms tend to have different areas well-ordered or disordered, and so complement each other in providing a complete structure of the protein.

The highest resolution (1.9–2.4 Å) structures have come from the yeast $P2_1$ and C2 crystals, bovine orthorhombic ($P2_12_12_1$) and tetragonal ($I4_122$) crystals, and *Rhodobacter sphaeroides* C2 crystals. Some crystal forms lack one small peripheral subunut: subunit 11(vertebrates) or QCR10 (yeast), and subunit 4 in *R. sphaeroides*. Since these subunits are not required for activity this probably does not detract from the usefulness for explaining function.

As mentioned above, the extrinsic domain of the Rieske ISP is found in different positions in different structures. Fig. 1 compares the ISP extrinsic domain's position and orientation in structures from each of the crystal forms with that of the beef tetragonal crystals in the presence of stigmatellin. Two crystal forms, the chicken orthorhombic ($P2_12_12_1$) and beef tetragonal, have an unfettered ISP allowing different positions or states of mobility to be observed in the same crystal form. Most of the highest resolution crystal forms have been obtained only with stigmatellin or similar inhibitor bound, which locks the ISP extrinsic domain in the "b" position. This precludes looking at different positions or mobility states (except by comparing these structures with those in other ISP states) or binding of Q_P inhibitors that do not maintain the b position. For example both yeast crystals are obtained with the aid of an anti-ISP Fv fragment which is intimately involved in crystal packing, and probably contributes to the good order and high resolution of these crystals [20]. The disadvantage is that presumably these crystals cannot be formed except when the ISP is in the b position. On the other hand the $P6_522$ beef crystal's crystal contacts involve the ISP in the c_1 position (Fig. 2), so these crystals cannot be formed with inhibitors that hold the ISP in the b position. Table 1 indicates which crystals have the ISP locked in the b or c_1 position and which have demonstrated potential for different positions.

Another important characteristic tabulated is non-crystallographic symmetry, or the contents of the asymmetric unit. The bc_1 complex apparently always exists as a dimer (homodimer of heteromultimeric protomers), and shows no tendency to monomerize except under conditions of extreme detergent concentration and ionic strength [21]. Any procedure to monomerize it is likely to destroy activity, as the ISP has its transmembrane helix associated with one monomer but functions with the other. An important question, which structures may help to answer, is whether cooperation between the dimers is important for function. When the enzyme crystallizes in a space group with proper two-fold crystallographic symmetry (such as $P6_522$, $I4_122$, or C2) the dimer axis is likely to be located on a crystallographic 2-fold so that the two monomers are crystallographically identical, i.e. the asymmetric unit of the crystal contains a monomer. When it crystallizes in a space group with no proper 2-fold (such as $P6_5$, $P2_1$, $P2_12_12_1$) then the 2-fold dimer symmetry becomes noncrystallographic and an independent structure is obtained for each monomer. If in fact there is asymmetry in the dimer then this is very important, not only because it lets you observe both structures, but because if crystallized with a monomer in the asymmetric unit, the asymmetric features would be averaged out in the single resulting electron density, making the interpretation difficult. To the extent that the dimer is symmetric, having a dimer still helps by increasing the ratio of data to parameters, since the number of unique reflections is proportional to the size of the asymmetric unit, while noncrystallographic constraints or restraints reduce the parameters by nearly half or serve as additional data, respectively. Crystals with more than one copy of the protomer in the asymmetric unit include the yeast $p2_1$, bovine orthorhombic, chicken orthorhombic, and beef P6 crystals (2 copies each) and *R. sphaeroides* $P2_1$ (4 copies) or C2 (6 copies!) crystals.

Availability of the diffraction data is a very important attribute of the structures because it allows those using the structure to make density maps for examining the reliability of features that may not have been described in the publication or for resolving conflicts between different models. The deposited pdb file is the crystallographer's interpretation of the electron density, further regularized and improved by a refinement program. In some places the interpretation may be absolutely clear and one can make out every atom, but in some parts of most structures the density is very unclear and the model is little more than the crystallographer's best guess as to how the protein may go. Furthermore crystallographic refinement techniques are steadily improving, and it is likely that applying new techniques to old data will provide new information about the structure and its dynamics. Already a project is underway to re-refine all of the structures in the PDB for which data is available, using today's best-practices methodology [22]. Since Feb 2008

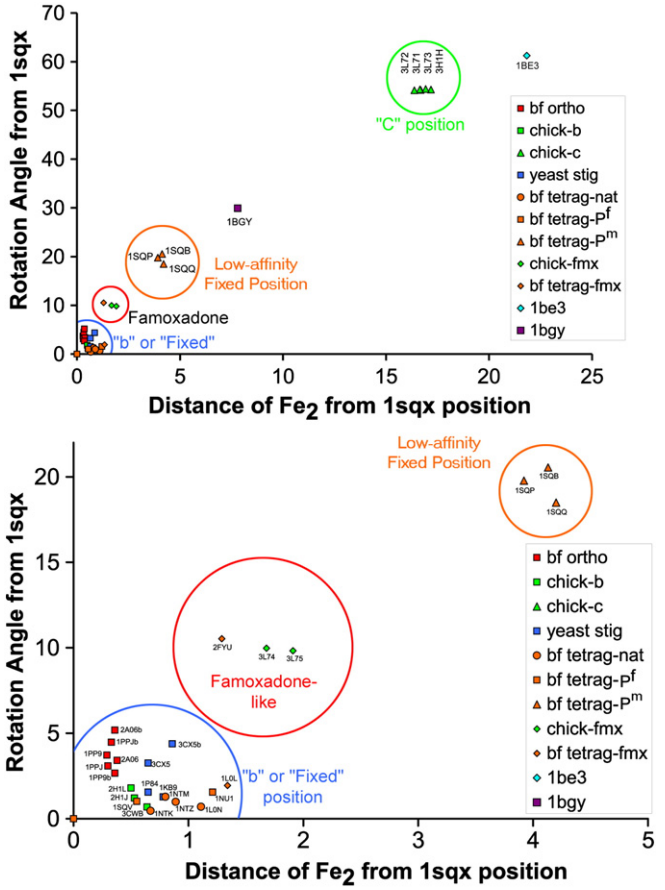

Fig. 1. Positions of the ISP extrinsic domain in different crystal structures. The position of the Fe2S2 cluster and the orientation of the extrinsic domain were compared to those in the presence of stigmatellin (structure 1sqx) to provide a 2-dimensional classification of the positions. Circles are from structures with no added inhibitors. Squares represent structures with stigmatellin, HQNO, nHDBT, or hydroxynapthoquinone. Diamonds are structures with famoxadone, fenamidone, or JG144. Triangles are in the presence of MOA-type inhibitors or triazolone compound. Color indicates the crystal forms: red, beef orthorhombic; orange, beef tetragonal; green, chicken; blue, yeast (two crystal forms). For the beef tetragonal crystal structures which contain a monomer in the asymmetric unit, the dimeric "biological unit" was generated using crystallographic symmetry. The structures were then superposed based on cyt *b* in one monomer before making the comparisons.

the Protein Databank has required depositors to submit the data on which structures are based, but many important bc_1 structures predate that requirement, and data is not available for some. It is to be hoped that the authors will eventually go back to find that data and send it in to the PDB, which will greatly enhance the usefulness of their deposition in the future.

For the most part the structures are in good agreement. It is amazing how little the catalytic subunits, excluding peripheral loops with flexibility or insert/deletions, differ between bacteria, fungi, and vertebrates. Even cyt $\mathbf{b_6}$ + subunit IV of the $\mathbf{b_6f}$ complexes is very similar to cyt *b*, especially on the P side of the membrane. Our purpose here is to focus on the differences between the structures, and on unexplained features. In some cases there are real differences that can tell us something, and in other cases it is just not clear what the true situation is. It is nice when several crystals corroborate the same story, but we actually can learn more when they differ, perhaps telling different parts of the same story. In other cases the situation may still not be clear in any of the crystals, and we should be aware of the uncertainty. It is important to know what you don't know! Of course there are many unanswered questions about the bc_1 complexes, so we have had to be selective and cover a few topics, mainly structural, where we are in as good a position as anyone, not to provide answers, but to provide some insight on the problems.

2. Questions about the mobility of the Rieske iron–sulfur protein

As mentioned above, the ISP is found in different position in different structures. Fig. 1 demarcates the different positions in a 2-dimensional plot, comparing the position in each structure with that in the tetragonal crystal in the presence of stigmatellin (1sqx). Some of the variability depends on the crystal form being used, and may reflect mainly crystal packing forces operating on the intrinsic mobility of the ISP. More significantly, in two different crystal forms in which the ISP is free to move, its extrinsic domain can be found in different positions, depending upon what is present in the Q_P site. These are the tetragonal ($I4_122$) crystals of the bovine complex [7], and the orthorhombic ($P2_12_12_1$) crystals of the chicken complex [8]. However results from these two crystal forms, while not contradictory, are somewhat different and have led to different paradigms to describe the mobility of the ISP extrinsic domain: the two-position model (distal/proximal or b/c_1 *positions* [8,23,24]) vs one based on occupancy (fixed, vs released or mobile, *states* [15,25,26]) from the tetragonal crystals.

The differences between observations with the bovine tetragonal crystals and the chicken orthorhombic crystals can be outlined with three questions. One thing is the same — the position of the ISP in the presence of stigmatellin or UHDBT is not significantly different in crystals of chicken, bovine, yeast, or bacterial bc_1 complex in different crystal forms. In other words, when the complex is in the fixed state induced by these or a few other inhibitors, the ISP is fixed in the same b position, regardless of the crystal form. So the first question, (1) "How do these inhibitors induce this position?" is not really a difference between crystals, but the way the results have been explained using the two forms. This will be considered in Section 2.1 below. A similar question applies to the fixed position induced by famoxadone and related inhibitors, which is significantly different from the b position (Fig. 1) and so might require a different explanation (Section 2.2).

(2) When the ISP is not in the b position or fixed state, the situation depends very much on the crystal form. In structures from the beef tetragonal crystals the ISP is modeled with the cluster ~4 Å away from its position in the b position, in what might best be called the "low-affinity fixed position". The occupancy (as judged by the anomalous peak due to iron) is low, so this represents a minority of the unit cells in which the ISP is in this position. The majority is really released, spread out over a continuum of different positions without enough occupancy in any one position to be crystallographically observable.

In several other crystals, the ISP is in a defined position with the cluster located within rapid electron transfer distance of cyt c_1. What is responsible for stabilizing the different c_1 positions, and which if any of these positions is relevant for the enzyme in the native membrane? And if there is a true c_1 position, why is it not seen in the tetragonal crystals? These will be considered in Section 2.3 below.

Finally, (3) what is the position/state in the absence of any inhibitor? In the chicken crystals it is the c_1 position, and is essentially unchanged when inhibitors favoring the c_1 position are added, but moves to the b position when inhibitors favoring that position are cocrystallized or soaked in. In the tetragonal beef crystals it is in the fixed position (although at low occupancy) and moves to the low-affinity fixed position, with even lower occupancy, upon binding of MOA inhibitors by the complex. This will be discussed in Section 2.4 below.

2.1. How do inhibitors hold the ISP extrinsic domain in the "fixed state" or "b position"?

The position seen in the fixed state of the tetragonal crystals (with stigmatellin or nHDBT) is essentially identical to the b position of the chicken crystals, and to the position seen in all other crystal forms with stigmatellin(yeast, bacterial) or nHDBT(yeast, bovine), as can be

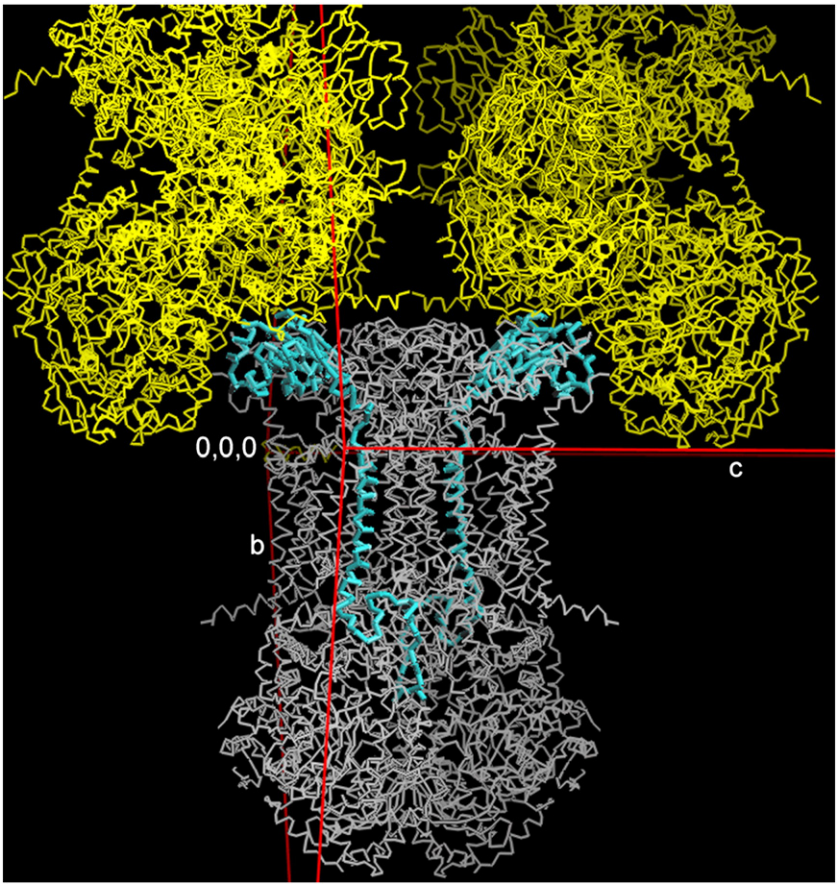

Fig. 2. Crystal contacts fix the ISP position in the hexagonal ($P6_522$) crystals. The principle inter-dimer contact is between the ISPs (blue) of one dimer and the core proteins of two other dimers (yellow). As a result changes in cell parameters due to dehydration or freezing result in slightly different positions for the Fe_2S_2 cluster. The asymmetric unit contains a monomer, so the two contacts depicted are identical by crystal symmetry, seen from opposite sides. Structure 1be3 was used for this figure. Figure made with O [88].

seen from Fig. 1. This b position is seen in chicken crystals with stigmatellin (3h1j), a Crocacin D analog(3cwb), or ascochlorin (3h1L), and in unpublished low-resolution structures (Huang and Berry) with alkylhydroxynapthoquinones and UHDBT. Thus there is good agreement about the structure in this state; the question is, how is it induced by these inhibitors?

There may be a link between the mechanism of these effects and the enforced bifurcation of electron transport at the Q_P site. The fixed state is presumably the state in which the ISP cluster is reduced by quinol at the Q_P site. This being the case, allowing or preventing binding in this position presents an attractive possibility for gating the reaction at Q_P to enforce bifurcation of electron transfer [15,25,27]. The different states seen with different inhibitors have been suggested to reflect the states in different stages of the reaction, allowing or preventing electron exchange with the occupant of Q_P [15].

Since the first detection of different positions or mobility states of the ISP, there have been two different explanations. They are not mutually exclusive, and perhaps neither can by itself explain all the phenomena. Zhang et al. [8] pointed out the H-bond between stigmatellin and the ISP cluster-ligand His161, and suggested this was responsible for the b position in the presence of this inhibitor. Fig. 3 shows this H-bond in structure 3h1j. The theory was further developed by Crofts and coworkers [28]. The ISP extrinsic domain is seen as freely diffusing within the limits of its tether, visiting different sites and occupying them in proportion to their stability, or binding constant. An H-bond from inhibitor to His161 was also seen with other inhibitors promoting the b position: nHDBT (1p84, 1sqv) and crocacin (3cwb). Inhibitors that promote the released state or c_1 position (myxothiazol, MOA-stilbene and other MOA inhibitors) bind more proximally in the Q_P site and do not come within H-bonding distance of, or project an H-bond donor or acceptor toward, the position of the docked ISP. The energy to break an H-bond varies, but a typical value is 5 kcal/mol, which is enough to make a 4000-fold change in an equilibrium constant. Thus formation of this bond when the ISP is in the b position could shift the equilibrium from the c_1 position to b position. Without the inhibitor the bond is not made, and the b position is less stable by this same factor.

In the same year, Kim et al. [25] proposed that conformational changes in the surface of cyt *b*, resulting from binding different Q_P-site inhibitors, were responsible for fixing the ISP in its docking site or releasing it in the mobile state. Further evidence for this came in 2002 when structures with an inhibitor of a new class was determined [29]. This was famoxadone, and it resulted in fixing the ISP at high occupancy near the b position, but did not form an H-bond with, or interact directly with, the ISP. A later, higher resolution structure from the same group (2fyu) with the structurally similar inhibitor JG-144, confirmed this fixation without H-bond, as did later structures with famoxadone and fenamidone in the chicken crystal form (3L74, 3L75).

We have argued [24] that the situation with these inhibitors is different from that with stigmatellin: famoxadone results in a significantly different position from the b position seen with stigmatellin or nHDBT, and while there is no H-bond from the inhibitor to the ISP, there is an H-bond from Y279 in cyt *b* to the same cluster-ligand His161 involved in the H-bond with b-position inhibitors. Still, the famoxadone-type inhibitors demonstrate that the ISP can be fixed near the b position in the absence of an H-bond from inhibitor to the ISP, and it is difficult to exclude that whatever is responsible for the position with these

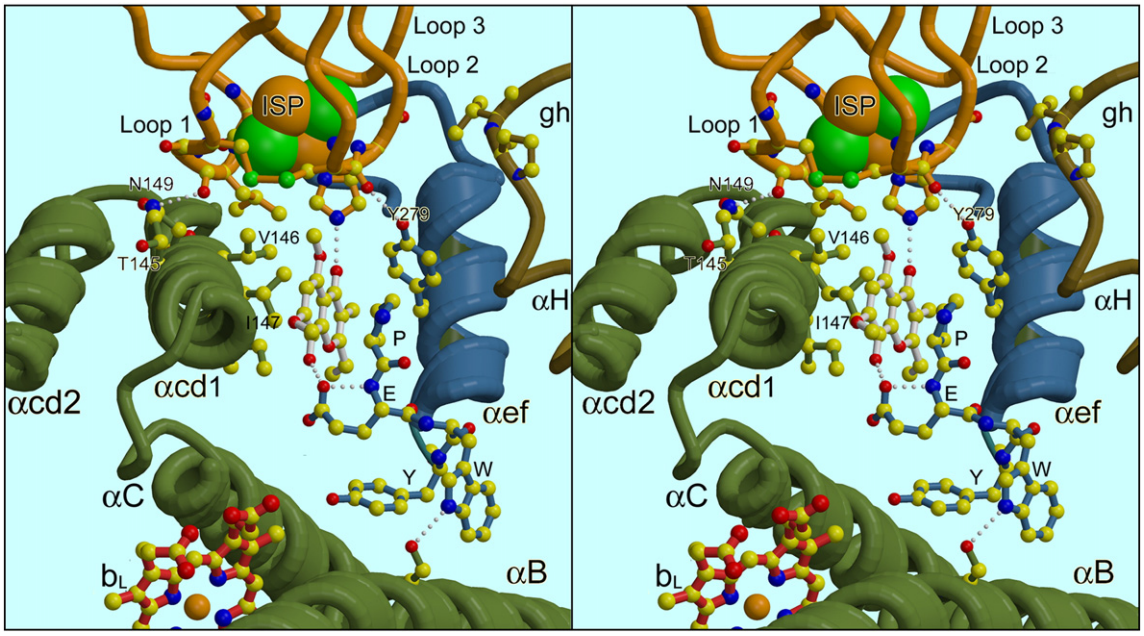

Fig. 3. Stereo view of stigmatellin in the Q_P site with the ISP docked in the "b" position. In structures with stigmatellin (shown here, central molecule with white bonds) or nHDBT, the ISP is in the "b" or fixed position, and there is a hydrogen bond between the inhibitor and cluster ligand His161 of the ISP. According to one hypothesis this H-bond is the factor which stabilizes the b position in the presence of stigmatellin. Cyt *b* is colored green except the ef-helix (blue) and PEWY segment (ball and stick with blue bonds). The ISP is in orange tubes with selected residues as ball and stick and the cluster as large balls. Note that the cluster is at a tip of the protein, surrounded by three "cluster bearing loops" of protein. All three loops contact cyt *b* in the b position, although most of the contacts are not shown here. Only loop 1 contacts cyt *b* in the c_1 position, as described in Section 2.3. b_H — high potential heme *b*. b_L — low potential heme *b*. From structure 3h1J. Figure made with Molscript [89] and Raster3D [90]. Stereo pairs for cross-eyed viewing are available in the supplemental materials for this and Figs. 6 and 10.

inhibitors may also play a role with the inhibitors that do form an H-bond. However we feel there is good evidence for a predominant role of the H-bond in fixing the position in other cases, as described below. Famoxadone and related inhibitors will be taken up as a separate case in Section 2.3.

Three further papers [29,26,15] explored the conformational changes in cyt *b* that seemed to correlate with mobility state of the ISP, and inhibitors which promote those states, classified as Pf favoring fixed state and Pm favoring the mobile state, in order to define the conformational switch. Large side chain differences in the ef loop residues 252–255 reported in Table 2 of the earlier paper [29], and explored by mutagenesis and ruthenium flash kinetics [30], were not confirmed by other crystal forms or by later, higher resolution structures from the same crystal form (e.g. compare 2fyu with 1ntm or 1ntz).

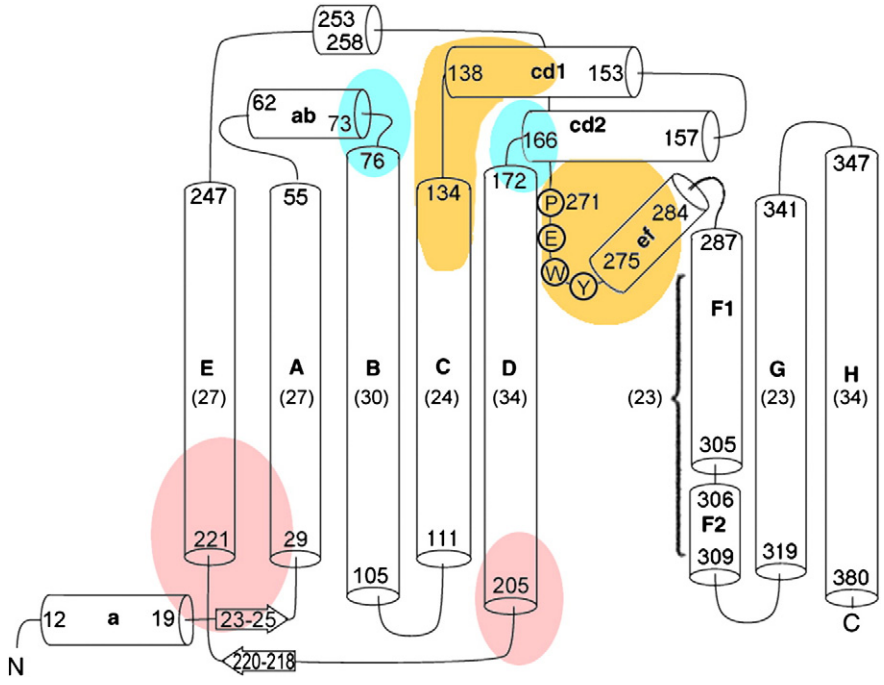

Fig. 4. Topology diagram showing the secondary structure elements of cytochrome *b*. Transmembrane helices are named with capital letters A–H. Other helices and loops are named with small letters corresponding to the transmembrane helices between which they occur. Residue numbers correspond to the chicken sequence. Shaded areas indicate residues involved in the Q_P site (orange), Q_N site (pink), and the "vise" which clamps the neck of the ISP, just below its hinge region, between the two monomers of cyt *b* (blue).

The later paper [15] used buried surface area and surface complementarity [31] to quantify changes in intimacy of the contact, but did not discuss differences in position of the ISP. The authors pointed out significant changes in conformation of cyt *b* in the PEWY sequence of the ef loop and in the cd_1 helix (The nomenclature of secondary structure elements is illustrated in the topology diagram for cyt *b* in Fig. 4). The former change was seen as not correlating with the type of inhibitor, and was attributed to widening of the Q_P pocket to accommodate either type of inhibitor. Movement in the cd_1 helix does correlate with the class of inhibitor, with Pf inhibitors displacing it in the proximal direction, and Pm distal, compared to the "native" structure. The cd_1 helix thus seems to be the best candidate for a conformational change gating the approach of the ISP extrinsic domain to its docking position at the Q_P site.

Fig. 5 illustrates the movement of the cd_1 helix, comparing structures with azoxystrobin, a Pm inhibitor, and stigmatellin, a Pf inhibitor, after superimposing the rigid transmembrane helices of cyt *b*. It can be seen that the cd_1 helix and the first cluster-bearing loop of the ISP, which is in contact with the cd_1 helix, move together in the same direction by about the same amount. More quantitatively, the Ca atoms of residues 142 in the ISP and 145 in the cd1 helix, which contact each other, move by 2.95 and 2.33 Å, respectively. The directions of their movement differ by only 14°. This gives the appearance that the cd_1 helix is being pushed down by the docking ISP or that it is moving down and allowing the ISP to follow, rather than moving aside and allowing the ISP to fall into the

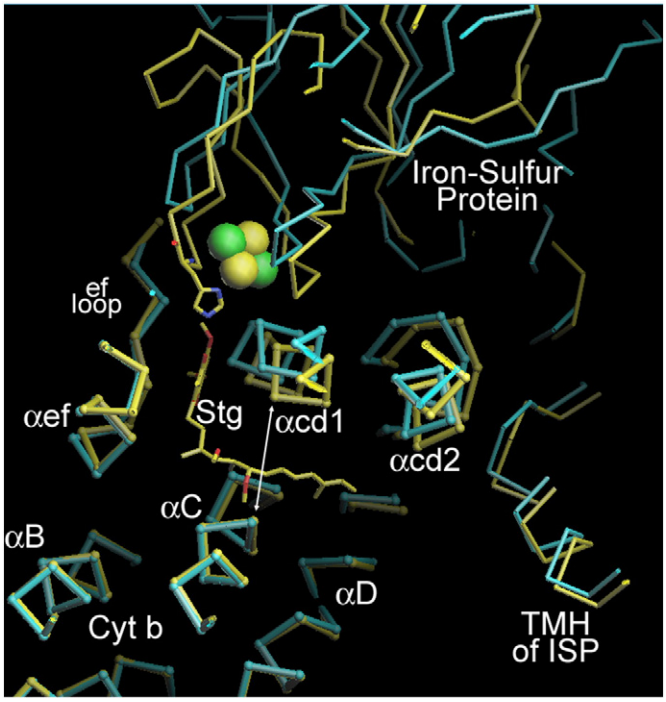

Fig. 5. Correlated movement of the ISP and the cd1 helix. Does the iron–sulfur protein push the cd1 helix down upon docking, or does the cd1 helix move downward to provide a favorable docking surface for the ISP? Comparing structures with stigmatellin (1sqx, yellow) and azoxystrobin (1sqb, blue) shows correlated movement between the ISP and the cd1 helix. The view is a slab through the bovine bc_1 complex showing the interaction of the ISP with the cd_1 helix. The orientation is from the opposite side as Fig. 3, so cluster-bearing loop 1 which contacts the cd_1 helix is on the right of the cluster. The protein is shown as C^{α} traces, with thin sticks for the ISP and balls and thick sticks for cytochrome *b*. The structures are aligned based on the transmembrane helices of cyt *b*, some of which are partly shown. When this is done the cd helices and the tip of the ISP are seen to be in different positions in the two structures. The Fe_2S_2 cluster (green and yellow spheres), His161, and stigmatellin (stg) are shown only for the stigmatellin-containing structure. The double-headed white arrow indicates the distance between C^{α}'s of residue 147 in the cd1 helix and residue 126 in transmembrane helix C (residues 146 and 125 in beef), which we use to monitor position of helix cd1 in the different structures. Note that cluster-bearing loop 1 of the ISP (just right of the cluster) moves nearly the same as the cd1 helix maintaining some of the contacts between them. Figure made with O [88].

binding crater as suggested by the schematic in Fig. 3 of [15]. For other views of this motion see Fig. 8 of [24], Fig. 2a of [15], and Fig. 5 of [32].

Unfortunately with the structures now available there is no way to tell whether (1) the cd_1 helix moves because of the inhibitor in the Q_P site, and allows the ISP to move closer; or (2) the ISP is docking for some other reason and exerting pressure on the cd_1 helix which causes it to move. Since the position of the ISP by definition correlates with the Pf/Pm status of the inhibitor, any conformational change in cyt *b* that correlates with the inhibitor status also correlates with the ISP position. Thus it is impossible to say whether the conformational change results from the inhibitor, or from the position of the ISP.

Comparing the structures with stigmatellin and azoxystrobin more carefully, it is seen that the movement in the first cluster-bearing loop of the ISP is a little greater than that of the cd_1 helix, making the contact tighter in the stigmatellin structure. For example Leu142 of the ISP and Asn148 (149 chicken) in the cd_1 helix make an H-bond of 2.8 Å in the stigmatellin structure, but 3.4 Å in the azoxystrobin structure. This seems more consistent with the ISP bearing down on the cd1 helix in the stigmatellin structure and easing up in the azoxystrobin. However the Azoxystrobin structure is, after all, the released or low-affinity structure, and we cannot exclude that the cd_1 helix pushes the ISP a short distance, then other contacts break and the ISP rests loosely on the cd_1 helix or even diffuses away resulting in the low occupancy. The movement of the cd_1 helix could be a passive part of the "spring loading" discussed in the next section, or it could be an active trigger to break whatever attractions are holding the ISP in its crater.

In the chicken bc_1 crystals, the same c_1 position is seen in the absence of inhibitors and with MOA inhibitors. And in this position there is no contact between the extrinsic domain and the cd_1 or cd_2 helices. So if the movement of the cd_1 helix is a result of pressure from the ISP, then adding MOA inhibitors should not induce any movement in the cd_1 helix in these crystals. That is in fact the case (Fig. 6 of ref [24]; compare native structures 3H1H, nt2, ant08a ~11.7 vs 11.5 Å for chicken or beef tetragonal crystals with MOA inhibitors 3L70 or 1sqb), but the argument is weakened by the fact that we don't fully understand the difference between the native state in the chicken vs tetragonal beef crystals, as discussed below in Section 2.4. If the native chicken crystals display the c_1 position because they are already in the MOA-induced state in the absence of inhibitor, then it could be argued that the cd_1 helix is already in its MOA-induced state. Still, this point is at least compatible with the ISP driving the cd_1 helix, whereas if we saw MOA-inhibitor-induced movement of the cd_1 helix in the absence of ISP contacts, it would be a strong argument for the inhibitor driving the cd_1 helix movement.

In principle, if we could prevent the ISP from interacting with the cd_1 helix at all, and look for movement in that helix induced by inhibitors, we should be able to answer the question. Experimentally this could be approached in at least three different ways. We could use a disulfide link to hold the ISP in the c_1 position as in ref [33], we could use a crystal form such as the $P6_522$ crystals where the ISP is constrained in the c_1 position by crystal contacts, or we could use an ISP-depleted complex with a functional Q_P site, which is available for the bovine [34–36], the *Rhodobacter capsulatus* [37,38], and perhaps yeast [39,40] bc_1 complexes.

In practice this is foiled by the extremely low affinity of the bc_1 complex for Pf-type inhibitors stigmatellin [36] and famoxadone in the absence of the ISP. This makes sense if you consider that the inhibitor-ISP complex is an analog of the substrate or product complex of the Q_P reaction, which seems reasonable at least in the case of stigmatellin or nHDBT. The phenomenon we are investigating, that binding of stigmatellin promotes movement of the ISP to the *b* position, is just an embodiment of the formation of that complex. The flip side is that movement of the ISP to the b position promotes tight binding of stigmatellin. Presumably many futile visits of each occurs before they arrive together and lock into the complex. In the case of stigmatellin, the obvious connection seems to be the H-bond:

the ISP provides an important part of the binding site for stigmatellin, and stigmatellin binding forms an H-bond that holds the ISP in that position. However since the same "mutual stabilization" occurs with famoxadone which does not form an H-bond, we are made to realize that the same thing could be achieved conformationally: If binding of either partner requires the same conformational change in cyt *b*, the energy required to induce that change would detract from binding energy. Binding of either would then promote binding of the other, and binding energy of both might be required to provide the energy requirement of the conformational change.

Although this blocks one path for answering the question, it provides us with a useful argument for testing residues for involvement in the capture of the ISP: any mutation which prevents the ISP from moving to the b position in the presence of stigmatellin or famoxadone would be also expected to prevent tight binding of the inhibitor, since that requires interaction with the ISP, presumably in the position normally induced by the inhibitor. We will use this in discussing yeast mutants where we do not have crystal structures with the inhibitors, to conclude that if the inhibitor still binds tightly, the mutation has not eliminated the mutual stabilization and thus the ability of the inhibitor to induce the fixed state.

In the case of stigmatellin, and nHDBT there is a strong body of indirect evidence that the H-bond between the Q_P-site occupant and His161 is the predominant force fixing the b position. This is based on the dependence of several phenomena on the redox state of the ISP. These arguments depend on the observation from high resolution structures of the ISP fragment [41] that there is no significant change in the protein structure with redox state of the cluster.[3] On the other hand there is very good evidence now that protonation state of His161 is redox-dependent, and so the strength of any H-bond formed with that residue may depend on the redox state of the cluster.

One such argument involves the effect of the inhibitor stigmatellin (or to a lesser extent nHDBT) on the E_m of the ISP. It has long been known that stigmatellin raises the midpoint of the ISP cluster by as much as 250 mV [42], with the result that addition of stigmatellin to the bc_1 complex leads to reduction of the ISP, even in the absence of any obvious reductant [43]. The classic explanation is that stigmatellin binds to the bc_1 complex about four orders of magnitude more tightly when the ISP is reduced. Knowing that the binding site for stigmatellin is in cyt *b*, with the only contribution of the ISP being the H-bond, and assuming no redox-linked structural changes in the protein, the simplest explanation is that the H-bond between stigmatellin and the reduced ISP is stronger by ~6 kcal/mol than the H-bond with the oxidized ISP (or if the H-bond with the oxidized ISP does not form, that ΔG for formation of the bond with the reduced ISP is ~6 kcal/mol). In the ISP depleted complex, stigmatellin binds very weakly if at all [36]. Putting these together with the fact that we are trying to explain, that in the presence of stigmatellin the ISP is found in the b position, it seems likely that all three phenomena (effect of stigmatellin on the midpoint potential, effect of stigmatellin on the ISP position, and effect of ISP on stigmatellin binding) are due to the strength of this H-bond between stigmatellin and reduced ISP.

The same argument goes for nHDBT, with the qualification that the effect on midpoint potential is smaller (consistent with weaker binding), and the lack of binding to ISP-depleted bc_1 has not been reported. Additional experimental results, including the effect of MOA inhibitors and "mobility mutants" on the E_m of the ISP, can be explained by assuming that ubiquinone binds with an H-bond to the ISP like stigmatellin and UHDBT, and binds more tightly when the ISP is reduced, raising its E_m [44,45]. Note that this is the condition (oxidized quinone and reduced ISP) giving rise to the epr $g_x = 1.80$ signal, sharpened and shifted to higher g values from the soluble ISP signal. The midpoint potential of the ISP in quinone-replete membranes is higher than that of the soluble fragment. MOA inhibitors such as myxothiazol lower the E_m of the ISP, although crystal structures show no contact. This could be due to their displacement of endogenous quinone, if quinone raises the E_m.

A series of mutations in the neck region of the ISP or the ef loop of cyt *b* results in "mobility defects" of the ISP in bacteria [46–50] and yeast [51]. These mutations affect the midpoint potential of the ISP in a way that parallels their effect on the equilibrium. Since the mutations are in cyt *b* or a part of the ISP distant from the cluster, they would not affect the intrinsic E_m measured in the isolated ISP fragment. Furthermore the effect on Em is nearly abolished in the presence of myxothiazol [47]. The most likely explanation [44,45] is that endogenous quinone binds more tightly to the reduced form in the b position, and that the oxidized form, lacking this stabilization, is predominantly in the c_1 position. Since tighter binding to the reduced form only occurs in the b position (where the ISP can interact with the quinone), the equilibria for movement between b and c_1 positions must be considered in calculating the effective E_m of the ISP. For the mutation-induced changes to modulate the effective Em of the ISP as observed, it has to be assumed that the oxidized ISP is predominantly in the c_1 position. Put another way, this means that ubiquinone induces the b position, but only if the ISP is reduced. This is consistent with observed redox effects on the ISP position monitored by EPR in oriented membranes [52].

Again, since the protein surface of the ISP is not affected by its redox state, the dominant force which specifically holds the reduced form in the b position must be the H-bond to the redox-sensitive cluster-ligand histidine. The mutation most favoring the b position (6Pro) raised the midpoint potential to 460 mV [48] compared to a value around 290 mV for the soluble fragment, implying that the reduced form is stabilized by 3.9 kcal/mol relative to the oxidized form. Since the ISP E_m in the wild-type bc_1 complex is only about 25 mV more positive than that of the soluble fragment, all but ~0.9 kcal/mol of this is cancelled out by the unfavorable equilibrium for attaining the b position in order to make the bond, in the wild-type complex. The most likely sink for this energy is the requirement to melt one turn of helix in the neck of the ISP in order to reach the b position [44,53–55]. The longer neck of the alanine insertion mutants and the low helical propensity of the proline or glycine mutants minimize that energy requirement. Thus the wild-type ISP is "spring-loaded" to facilitate dissociation of the product complex [44]. Although the equilibrium for the reduced ISP is toward the b position, it can be surmised from the rate of re-reduction of ruthenium-flash-oxidized cyt c_1 that reduced ISP is leaving the Q site at a rate near 16,000 s^{-1} in the wild-type complex [56], if it is assumed that most of the reduced ISP in this experiment is docked at Q_P, bound to oxidized quinone before the flash. This is considerably faster than the steady state turnover of the complex or the flash-induced reaction-center driven Q_P-site reaction, and so is not a rate-limiting step. In a proline neck mutant, this rate became very slow (25 s^{-1}) with an increased activation energy, and became the rate-limiting step. According to the "spring-loaded" description of the mechanism, this would be because the spring was drastically weakened by replacing two high-helical-propensity alanine residues with helix-breaker proline, and the increased activation energy corresponds to the energy to dissociate the product complex with less aid from the spring.

Presumably the oxidized ISP binds tightly to the Q_P site with quinol present to form the reactant complex, but this is hard to access experimentally due to the instability of that redox combination (oxidized ISP and reduced ubiquinone). However from the offset in rate of the bifurcated reaction as a function of Eh from the midpoint potential of ubiquinone in the membrane, or from the offset of pH dependence curve from the pKa known for the soluble Rieske fragment, it has been estimated that the oxidized ISP binds ubiquinol 14 times more tightly [57]. Such preferential strong binding of reaction partners in the "allowed" forward and reverse reactions may contribute to a double-gating mechanism to prevent bypass reactions [58].

[3] The authors qualify this by observing that it is difficult to be certain that the ferricyanide-treated sample was not reduced by radiation during data collection.

In addition to the neck insertion or low helical propensity substitution mutants that increase the midpoint potential, some mutations in the ef loop and "box 1" of the ISP lower the midpoint potential. The effect is additive with that of the neck mutants: L286F lowers the E_m by 50–60 mV in wild type or in insertion mutants with E_m's elevated by 60 or 100 mV [48]. We attribute this to stabilization of the c_1 position by the mutation. In the c_1 position, which will be described in the next section, there is a thin line of contact between the first cluster-bearing loop (which includes Box I) of the ISP and the most distal portion of the ef loop of cyt *b*, with probably two H-bonds and several van-der-Waals contacts. Any mutation that stabilizes this contact could shift the equilibrium toward the c_1 position. Mutations of this type arise as revertants to the neck mutations that stabilize the b position, suggesting the need to keep this equilibrium within a certain range. And the mobility mutants in the ef loop reduce or prevent the interaction of the ISP with quinone as observed by EPR spectroscopy, consistent with shifting the equilibrium so that even the reduced ISP spends most of its time in the c_1 position.

In this we are assuming that the mobility mutations affect the equilibrium between the b and c positions, which is only a hypothesis. However it seems to be the simplest way to explain the various observations with these mutations, especially the compensatory effects of neck and ef-loop mutations and the fact that the 6-Gly and 6-Pro substitutions had essentially the same effect. These two mutations were designed to have the opposite effect on neck "flexibility". The finding that increased rigidity and increased flexibility had similar effects, and both could be partially overcome by a decrease in neck length, is hard to explain any other way. In fact no special flexibility is required of the hinge — the flexion is spread out over four residues, and does not require any $\phi - \psi$ angles prohibited for general residues. One thing Gly and Pro have in common is low helical propensity, which would reduce the energetic cost of melting the helix to allow approach to the b position. And the additive effects of neck and ef-loop mutations on the ISP E_m is nicely explained by assuming they both affect the equilibrium between b and c_1 positions.

The H-bond with Q cannot be the whole story, though, because 1) the neck insertion mutants still raise the midpoint potential slightly in the presence of myxothiazol [47], or with the Q-pool extracted [59], and some ef-loop mutants (RcT288S) [49] lower the potential even below that seen in wild-type with myxothiazol. This suggests that the b position still stabilizes the reduced form of the ISP more than the oxidized when the Q_P-occupant cannot H-bond the ISP. Perhaps some residue of the protein, such as Y279 (302), can form a much weaker redox-sensitive H-bond. Perhaps such interactions could account for the difference between the EPR spectrum of the soluble fragment and that in the presence of myxothiazol, especially with the neck-relaxing mutants (Fig. 1b of [47,59]).

2.2. How do famoxadone and related inhibitors, which do not form an H-bond with His161, fix the position of the ISP?

Famoxadone [26,29] and structurally related JG144 [15] and fenamidone [24] fix the ISP at high occupancy near the b position. Famoxadone binds very weakly to the ISP-depleted bovine bc_1 complex as judged by red-shift titration, with half-maximal effect around 30 μM (LSH and EAB, unpublished observations). This suggests a mutual stabilization interaction, with famoxadone stabilizing the ISP in the famoxadone position and the ISP (in the famoxadone position) stabilizing the binding of famoxadone, but without any direct physical interaction to explain the effect.

The position is significantly different from the fixed position with stigmatellin or UHDBT, with the Fe_2S_2 cluster about 1.5 Å farther from cyt *b* and the extrinsic domain rotated 10° relative to the position with stigmatellin (Fig. 1 and [24]). And although there is no H-bond from the inhibitor to the ISP, there is an H-bond from Tyr279 of cyt *b* to His161 in the presence of these inhibitors.

We considered the involvement of Y279 in a previous paper [24]. Certainly the H-bond must stabilize the famoxadone position. But for it to be triggered by famoxadone binding would require conformational coupling between the binding site and y279, in which case the "H-bonding" and "conformational switch" hypotheses start to merge. As discussed in that paper, famoxadone could either stabilize the H-bond from Y279 to the ISP, or it could destabilize a competing intra-subunit H-bond with Ile269. The binding site of famoxadone is more like that of the MOA inhibitors than like stigmatellin, being more proximal and involving an H-bond from a carbonyl O of the inhibitor to the backbone N of Glu272. Interestingly, mutation of Y279 to Asn, Gly, Ala, or Ser results in resistance to myxothiazol but not to stigmatellin, despite the distal location of Y279 [57,60]. However mutation to Phe did not give resistance, so the H-bond must not be important for this effect.

To test the involvement of Y279 H-bond for the famoxadone effect, we created the mutant Y279F in *Saccharomyces cerevisiae* (DeBari, unpublished). As previously reported for the equivalent mutant in bacteria [57,60], the bc_1 complex was functional. We have not yet developed a crystallization protocol for the yeast bc_1 complex, so we determined affinity for famoxadone as a measure of the mutual stabilizing interaction. The mutant IC_{50} was 2- to 3-fold higher than wild-type, implying that the Y279 H-bond contributes some to the mutual stabilization. This effect is small compared to the ~30-fold decrease in affinity for famoxadone seen with the ISP-depleted complex. While that work was underway it was shown that mutation of the corresponding residue in *R. capsulatus* does not lead to famoxadone resistance [60]. Thus presumably the ISP is still held in the famoxadone position in the absence of the H-bond to it from Y279, and this residue is not responsible for the effect of famoxadone on the position of the ISP. It may be that no one residue or effect is, but rather a large number of small effects including that of Y279.

Like the MOA inhibitors, famoxadone must exclude ubiquinone from the site, and so we would expect the same slight depression of the midpoint potential of the ISP if there is no preferential binding of one redox form. The effect of famoxadone on the E_m has been determined indirectly by its effect on the equilibrium between cyt c_1 and the ISP, and compared with the value with MOA inhibitors azoxystrobin and MOA-stilbene using the same method [26]. In fact the E_m with famoxadone is about 50 mV higher than with the MOA inhibitors, implying tighter binding of the reduced form. Again assuming only the H-bonds to cluster-ligand histidines are redox-sensitive, and noting that in the famoxadone position His161 H-bonds Y279 of cyt *b*, we would be forced to conclude that this bond is stronger with the reduced ISP. It would be useful to test the effect of famoxadone on the E_m of the ISP with the Y279F mutant.

2.3. Why do we see "distal" or "c" position(s) in some crystals, but the "released" or "mobile" state in others?

This is the main difference that leads to the two different paradigms for the two crystal forms that allow movement of the ISP. In some crystals, including the chicken orthorhombic crystals, the ISP can be found in a defined position that places the cluster near cyt c_1. This c_1 position of the ISP varies depending on the crystal form. To a large extent the differences in c_1 position may be attributed to different crystal contacts, and it might be argued that there is no true c_1 position and the positions seen are due to artificial stabilization by crystals contacts. We believe that there is one c_1 position relevant for the native enzyme, but that it is rather tenuous and subject to being modified by crystal packing forces.

The position of the ISP found in chicken crystals with bound MOA inhibitors is labeled in Fig. 1 as the c_1 position. Hexagonal ($P6_522$) crystal 1be3 has the extrinsic domain rotated even farther from its b position, which brings it close enough to cyt c_1 for an H-bond between a heme propionate and His161 [9]. Crystals of bovine or

rabbit bc_1, in this crystal form collected near room temperature, fall in between (Fig. 2 of [32]).

However, in the $P6_522$ crystal form, the main crystal contact connecting dimers in the lattice involves an ISP extrinsic domain of one dimer inserted in the depression between Core proteins of another dimer (Fig. 2). Thus changes in cell parameters due to dehydration and cryocooling will affect the forces exerted by the crystal contact, and may account for the different positions seen with this crystal form, and perhaps none of the positions seen with this form represents a particularly stable position for the ISP in the native complex in the membrane.

The orthorhombic crystals of chicken bc_1 with the ISP in the c_1 position (PDBID 3L70 through 3L73) are affected by crystal contacts to a lesser extent, if at all. There is a possible interaction between Asp190 in the ISP of the second monomer (chain R) with Lys77 in subunit 6 (chain S) of another dimer. Both side chains are disordered so it is impossible to say whether they are arranged to form that salt bridge, but the ISP of chain R has somewhat lower B-factors and higher occupancy than that of NCS-related chain E, and that may result from stabilization by this contact. Nonetheless the position of chain R is essentially the same[4] as that of chain E which makes no contacts, and both move to the b position when the crystals are soaked with stigmatellin (neither chain has a crystal contact in the b position), suggesting that the crystal contact has little influence on the position of chain R. Occupancy ranges from 0.85 to 0.93 for chain E and 0.90 to 0.98 for chain R in the four structures mentioned, so the ISP is in this position in the great majority of asymmetric units, but with relatively high thermal displacement: average B- factors for protein atoms in residues 73 to 196 are 146 to 164 $Å^2$ for chain E and 104 to 124 $Å^2$ for chain R. Due to partial occupancy in the major position and/or high B-factor, the ISP extrinsic domain is poorly ordered. The disordered electron density was the first indication of mobility of the ISP [7].

In the tetragonal crystals co-crystallized with inhibitors of the Pm class (MOA inhibitors) the occupancy judged by Fe anomalous peak is low, signifying the majority of the ISP is distributed over a range of positions too thinly to be seen in the electron density. This is the "released" or "mobile" state, where of course "released" and "mobile" refer not to the modeled position but to the majority of the ISP which is not seen because it is dispersed.

The authors emphasize the occupancy, i.e. the amount of ISP remaining fixed, with little discussion of the exact location at which it is fixed. The ISP is modeled in all of the deposited structures for this crystal form, and comparing the different structures from this space group with each other and with structures from other crystal forms, it becomes clear that while the structures with Pf inhibitors have the ISP fixed in the same b position as structures with Pf inhibitors in other crystal forms, the low-occupancy ISP in the released state is modeled in a significantly different position, which we have called the "released" position [24]. It might better be called an alternate, less stable, fixed position from which most of the ISP escapes to the truly released positions, so we have labeled it "low-affinity fixed position" in Fig. 1.

However the important thing here is not that there is an alternate, less stable fixed position near the b position, but that there is not a stable position near the c_1 position to capture the ISP when the b position becomes unavailable. Below we examine the c_1 position in crystals that do exhibit it, consider what stabilizes it and whether it depends on crystal contacts that may not be present in the tetragonal crystals.

Before going on, though, it is worth pointing out that in some cases, the c_1 position has been observed in the tetragonal crystals. In the 1998 paper [25] it was reported that co-crystallizing with MOA-stilbene "abolished the anomalous signal for the FeS at the position observed in the native crystals … a minor peak appeared closer to cytochrome c_1". And this "appeared consistently in all forms of MOA-stilbene containing crystals". This peak is depicted in the anomalous difference map, Fig. 3A of [25]. The peak attributed to ISP cluster there appears to be precisely where it is in the chicken c_1 position (The apparent difference between that figure and Fig. 6a of Zhang et al. [8] is due to different rotation about the dimer axis). However the significance of this peak was downplayed in the discussion due to low occupancy in that position, and when a structure with MOA-stilbene (1sqq) did come out (based on data collected after the first paper appeared) it had the ISP in the low-affinity fixed position (near the b, not c_1 position). Thus the difference may not be absolute but may result from a delicate balance between the released and c_1 position, depending on pH and ionic strength of the crystallization solution and crystal packing forces.

What stabilizes the c_1 position in the chicken orthorhombic crystals? If the ISP extrinsic domains in the chicken crystal make no contacts with other dimers, the c_1 position must be stabilized by contacts within the dimer, which would in principle be relevant for the native enzyme in the membrane. When it is in the c_1 position, the main contact between the ISP extrinsic domain and the rest of the complex is between the first cluster-bearing loop of the ISP and the ef loop of cyt *b*. Beside that there is only the neck region which tethers the ISP to the transmembrane domain of the complex, Lys94 which may make an H-bond to cyt *b*, and in some cases there is the above-mentioned H-bond with the cyt c_1 heme propionate.

Fig. 6 shows the details of the interaction of the ISP in the c_1 positions with the ef-loop, in hexagonal ($P6_522$) crystals (Fig. 6A, from 1be3) and the chicken orthorhombic crystals (6B, 3L71). Seen from this angle, the ISP seems to be perching on the ef loop. As seen in the chicken structure of Fig. 6B, the side chains of Leu263, Val264, Thr265, and Pro267 extend horizontally on either side of the backbone, while Pro266 extends downward, leaving a relatively flat, broad upper surface for the ISP to rest on. Likewise on the ISP Leu142 and Cys144 extend horizontally, with Gly143 between, permitting the backbones of the two stretches to come together. Fig. 6C identifies the specific contacts involved. There are two potential H-bonds between the two: 265N in cyt *b* with 142 O in the ISP, and highly conserved Thr265 in cyt *b* with a backbone N on the ISP.

As discussed in the previous section, mutations in this part of the ef loop and the first cluster-bearing loop of the ISP result in ISP mobility defects that seem to affect the equilibrium between c_1 and b positions. This lends credence to the idea that this contact is involved in the c_1 position of native cyt bc_1 in the membrane, and not an artifact of these crystal forms. The residue Thr265 involved in both of these contacts is highly conserved. Mutations of this residue (288 in *Rhodobacter*) result in loss of activity or decreased activity due to "mobility defect" of the ISP.

Fig. 6C shows the same view as 6b rotated 90° so that the contacting backbones are in the plane of the picture, to identify the contacts. Although the ef loop looks very unsupported in this format, in fact it is wrapped securely around Gln138 and supported by that residue and Trp142, with many H-bonds to those residues and others at the beginning of the cd1 helix.

What is different in the 1be3 structure, which has the cluster closer to cyt c_1 allowing an H-bond between the cluster ligand H161 and heme propionate of cyt c_1 [9]? Fig. 6A shows this most extreme c_1 position, for comparison with the chicken structure in Fig. 6B. In both panels the ISP cluster-bearing tip is facing toward us, a little to our left. In A the 1be3 structure is rotated farther to the left, bringing the cluster closer to heme c_1. The ISP overhangs the contact with ef that we have been discussing. Note that the carbonyl O of 141 (white arrow) is well to the right of the ef loop in panel B but a little to the left in panel A, where it is H-bonding Thr265 (264 beef) which has rotated about its backbone to face upward towards the ISP. Val264 becomes Asn263 in beef. This residue projects toward cyt c_1 and could potentially make an H-bond with the forward leaning ISP loop 1 of this crystal, although that bond is not made in the deposited coordinates. If so this amino acid

[4] Superimposing the cyt *b* monomers on each other superimposes the IS cluster within 0.88 A and the ISP with an angle of 3.8°.

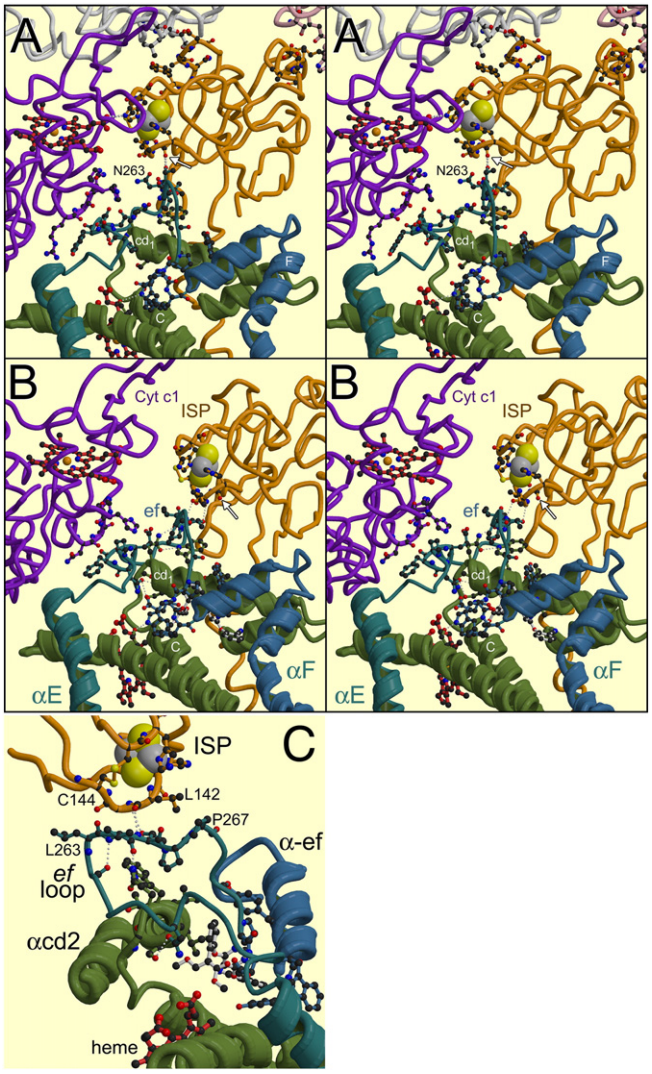

Fig. 6. Underpinnings of the c_1 position. In the c_1 position, loop 1 of the ISP rests on the top of the ef loop. These contacts presumably are responsible for fixing the c_1 position in the absence of crystal contacts, as in chicken crystals (B, C; structure 3L71). In the hexagonal beef crystals (A; stereo view; from structure 1be3), the ISP is contacted by core proteins of another bc_1 dimer, visible along the top of the fig. in gray (left) and pink (right), which may be responsible for its different positions. Cyt c_1 (magenta) is on the left with its heme propionates extended toward the ISP (orange protein; cluster with yellow and grey sulfur and iron atoms). Cyt b is below in various shades of blue and green. The arrow indicates ISP:141 O to dramatize the difference in relative positions of the ISP and cyt b in the two structures. Figure made with Molscript [89] and Raster3D [90].

difference, as well as the crystal contacts, could be responsible for the cluster in 1be3 being closer to cyt c_1. Finally, Leu263 (chicken sequence) contacts Val138 on the descending branch of the first cluster-bearing loop; the other side of the loop from the residues discussed so far.

What does the "neck" region tell us about the position of the ISP in the two crystal forms? As described above in connection with the spring-loading, approximately one turn of helix in the neck region melts when the ISP goes from the c_1 position to b position. What does it look like in the low-affinity fixed position seen in the released state? The neck is nearly identical to that in the c_1 position. This appears to say that the helix melting occurs during the movement from the low affinity fixed state to the b position, not during the much larger motion from the c_1 position to the low-affinity position. This would imply that the "spring-loading" only serves to pull the cluster away from Q_P by 4 Å — enough to break the strong hydrogen bond in the product complex.

Why is the c_1 position not stabilized in the same way in the tetragonal crystals when the fixed position is not available due to binding a Pm inhibitor? There could be a crystal contact in the tetragonal crystals that prevents the ISP from achieving the c_1 position, or destabilizes the c_1 position. In those crystals with the shortest c axis there is some contact between the Lysines 103 and 104 in the helix on the top of the ISP with the Core 2 protein of a symmetry-related molecule in the next layer. In 2fyu (famoxadone fixed position) there is a strong (2.82 Å) H-bond from the side chain of Lys103 in the top of the ISP extrinsic domain to backbone oxygen of residue 349 in Core 2 of another monomer.

In the crystals with Pm inhibitors (1sqb, 1sqp, and 1sqq) the rotation of the extrinsic domain brings Lys 103 and 104 into interaction with residues 351 and 352 in the same Core 2 protein. This contact could be responsible for stabilizing the "low-affinity fixed position". If the occupancy in the low-affinity fixed state is low as inferred from anomalous peak height, the ISP must not be very strongly fixed by this interaction. However if the anomalous peak is low because of high B-factor in the undocked cluster tip, and occupancy is actually high; it could be that this interaction is holding the protein in this conformation and preventing it from moving to the c_1 position.

To see if crystal contacts would interfere with the c_1 position as seen in the chicken crystals, one can superimpose chicken structure 3L70 (in the c_1 position) with 2fyu based on cyt b. In the resulting c_1 position the contact with the next layer did become closer, with 2.07 Å between C^{α} of residue 104 in the ISP and N of 354 in Core 2 of the symmetry-related monomer. It is not clear that this would destabilize the c_1 position however, as the flexibility of the protein might be expected to absorb the clash and the contact might actually stabilize the c_1 position, possibly in a slightly different position due to the contact as in 1be3.

The difference could also be a species difference, since the c_1 position of an unfettered ISP has been seen only in the chicken crystals, and the released state only in bovine. Since the unfettered chain E is less than 100% occupied in the chicken c_1 position, and the bovine crystal in the released state can show significant accumulation in this position under some conditions (Fig. 3a of [25]), it may be that a slight change in the energy balance due to an amino acid change could make the difference, as could a difference in pH or ionic strength of crystallization. Based on the procedure described [7,61] for the tetragonal crystals, the final ionic strength and pH before vapor diffusion would be 0.265 M and 7.2, compared to 0.1 M and 6.8 for the chicken crystals. And the early report of a tetragonal c_1 position with MOA-stilbene may have been from while the procedure was still evolving, with slightly different conditions allowing observation of the c_1 position. If one of the ef-loop mobility mutants that depress the E_m of the ISP by stabilizing the c_1 position could be crystallized (*Rhodobacter* or yeast) it would be expected to show a c_1 position. On the other hand the neck mutant +2ala should allow the complex to be crystallized without stigmatellin in the forms requiring the b position, and might well allow visualization of the tightly bound ubiquinone at the Q_P site if our ideas are correct.

2.4. What accounts for the different behavior of the ISP in the absence of inhibitor, in the tetragonal beef crystals vs chicken crystals?

What state or position prevails in the absence of inhibitor? If we go by position, the uninhibited chicken crystals are in the same state as with Pm inhibitors, in the c_1 position. Thus it is the Pf inhibitors that have a big effect, moving to b position, while Pm inhibitors have no effect on position but increase occupancy at the c_1 position slightly. Conversely, the tetragonal crystals in the absence of inhibitors have the ISP in the same position as with pF inhibitors, the b position (but at low occupancy), and Pf inhibitors increase the occupancy with almost no movement, while Pm inhibitors cause movement ~4 Å to the low-affinity position with even lower occupancy.

This is a different question than the previous one about the position in the presence of Pm inhibitors. However the explanation may lie in the same fact that the chicken crystal has a stable c_1 state — regardless

of whether it is an artifact stabilized only in the chicken crystals by crystal packing forces, or a true physiological c_1 state that for some reason is not reached in the tetragonal crystals. In the absence of inhibitors the c_1 position could be most stable in those crystals where it is available, followed by the fixed b position, followed by low-affinity fixed position. Pf inhibitors stabilize the b position making it even much more stable than the c_1 position, so lead to b position in both. Pm inhibitors destabilize the b position, so the chicken crystals remain in c_1 position, while tetragonal crystals move from b to low-affinity fixed position.

That picture is not very consistent with the H-bond explanation and especially the spring-loading concept, which predicts the spring loading will make the b position very unstable unless there is a good strong H-bond to compress the spring and hold the ISP in the b position. To explain partial occupancy of the b position in the absence of inhibitors with this hypothesis we have to propose that something, perhaps endogenous ubiquinone, is bound at a minority of Qo sites and makes the H-bond to hold the ISP in the b position. It need not be that the tetragonal crystals have more ubiquinone than the chicken ones. Assume that in both crystal forms less than half of the Qo sites have ubiquinone bound. In the tetragonal crystal, those without ubiquinone have the ISP "released" and invisible, so the crystals show the minority bound to sites with ubiquinone. In the chicken crystals that minority bound to sites with ubiquinone is overwhelmed by the majority in the c_1 state, so the latter gets built in the model. Adding Pm inhibitors displaces the quinone and releases more ISP to go to the c_1 position, increasing occupancy (compare occupancy of structures 3L70, 71, 72 with native structure 3H1H: 0.93, 0.91, and 0.88 vs 0.80 for chain E, and 0.98, 0.98, 0.95 vs 0.85 for chain R).

This may not be a very tenable explanation for several reasons. First, there may not be enough ubiquinone in the preparations to occupy a significant fraction of the Q_P sites. It was reported that the bc_1 preparation used for crystallization contained 0.74 mol Q per mol cyt c_1 [7,61], but since quinone is seen at the Q_N site, a good fraction of an equivalent must be there. Second, if the crystals have been treated with oxidant such as ferricyanide, or crystallized in its presence, this should eliminate the fixed position just as Pm inhibitors due, since we concluded above that the oxidized ISP does not bind quinone. On the contrary, structure 1ntm which was fully oxidized before harvesting had a higher Fe_2S_2 cluster anomalous peak than 1ntz, in which cyt c_1 was partly reduced (Both are at the fixed, or b, position)[62]. Possibly photoelectrons from the X-rays rapidly reduced the ISP. Third, if endogenous ubiquinone is responsible for holding the ISP in the fixed position without inhibitors, treating with excess quinone should increase the amount in the fixed position, and perhaps allow visualization of quinone at Q_P in a reliable way. This must have been tried many times but no such result has been reported.

3. Does residue Y132 move upon binding nHDBT?

The importance of this highly conserved residue was shown by Saribas et al. [63] who mutated the corresponding residue (Y147) in *R. capsulatus*. Mutation to F, L, or V had minor effects while A or S severely inhibited the complex. The mutants had normal occupancy of the Q_P site by quinone and stigmatellin, and normal interaction of the ISP with these as judged by EPR. Only the rate of oxidation of quinol was affected. Similar results were obtained in yeast by Wenz et al. [64]. The Y132 OH group is involved in a putative H^+ exchange pathway, which could account for the ~2-fold decrease in activity of Y132F, but apparently this role is not necessary for activity.

Y132 does not vary significantly in position in the X-ray structures with various inhibitors, except for 1sqv with UHDBT [26]. In this structure Y132 (Y131 in beef) has swung around to direct its OH at the inhibitor, forming an H-bond with a keto group of the inhibitor (Fig. 7B). An earlier structure of an alkyl-HDBT-inhibited yeast bc_1 complex is modeled with Y132 in the conventional place. This is 1p84, yeast bc_1 with heptyl-HDBT [65]. The binding is much like that of stigmatellin except that E272 carboxylate does not H-bond the inhibitor. A water molecule is bridging between the inhibitor and E272N, in much the same position as the carboxylate in most structures with stigmatellin. Does the conformation depend on species, the length of the inhibitor tail, or perhaps on the crystallization conditions? The yeast structure is somewhat higher resolution (2.50 vs 2.85 Å). Unfortunately data was not deposited for either structure, which precludes independent evaluation of the density, or modeling each as in the other and refining to allow for model bias. We have a low resolution (3.2 Å) dataset of chicken bc_1 with UHDBT bound, which we modeled as in the yeast structure. In one of the monomers there is a blob of unaccounted density in the position of the tyrosine ring of the bovine structure (Fig. 7B). We believed this to be a cluster of water molecules or even just noise, especially since density in the corresponding place in the other monomer is weaker. However modeling as in 1sqv and refining (Fig. 7C), the resulting density is somewhat consistent with that model. At low resolution, model bias is more of a problem. Based on this data we would not propose an alternate position for Y132, but we could not rule it out. Data on nHDBT-resistance of the Y132 mutants would be useful.

4. What is the significance of the *cis*-peptides at the beginning of transmembrane helices C, E, and H of cytochrome *b*?

As of 1999, 5.7% of Xxx-Pro peptides in the PDB were in the *cis* conformation. Cyt *b* contains 20–30 prolines (19, 21, 25, 28, 29) for yeast, beef, chicken, and *R. sphaeroides* and *capsulatus*). And thus it is not very surprising that cyt *b* contains 2 or 3 *cis* peptides. However it is interesting to note that they are highly conserved and thus likely to be important for proper folding of cyt *b*, and to speculate about their role in the folding process and the possible involvement of prolyl isomerases in cyt bc_1 assembly.

There are three locations in cyt *b* that generally contain *cis*-peptides, with the second (i+1) residue of the peptide (usually Pro) corresponding to yeast residues 109 (at the beginning of helix C), 223 (at the beginning of helix E), and 347 (at the beginning of helix H) in *S. cerevisiae*. All three of these are *cis*-peptides in all bacterial structures solved to date, e.g. *R. capsulatus* (1zrt;), *R. sphaeroides* (2qJy etc.), and *P. denitrificans* (2yiu). The numbering is the same in all three, the *cis*-peptide i+1 residues being P124, P246, and P/I388.

Vertebrates and other metazoans have a two-residue deletion in cyt *b* which removes the two residues making the *cis*-peptide at the beginning of helix C, and there is no *cis*-peptide near there in the available vertebrate structures. The bc loop is very short, and the deletion just makes the turn tighter in vertebrates, with the 4 residues 107RSPR of yeast cyt *b* being replaced by two, 109CF, in chicken.

Residue 223 is a highly conserved Pro in most organisms but mutated to Ser, Gly, or Asn in some Saccharomycetales; in *S. cerevisiae* it is Ser. This is a *cis*-proline in all non-saccharomycete structures available. Although the peptide His222-Ser223 has been modeled as *trans* in yeast structures to date, examination of the electron density and difference maps calculated with the high-resolution structure 3cbx, and further refinement after changing the model, clearly show that there is a *cis* peptide between His222 and Ser223 (Fig. 8a and E.A.B., unpublished). An interesting mutation converting Ser223 to Pro in *S. cerevisiae* will be discussed in the next section on function of the Core proteins.

A similar case is found with the residue at the beginning of helix E. This is Pro347 in yeast, is a *cis*-proline in available bc_1 structures, and is conserved in mitochondrial (except some fish and sea urchins) and most bacterial cyt *b*. However in a few Rhodobacteracia such as *Paracoccus* and *Bradyrhizobium* it is Ile. In structure (2yiu) this residue (I388) is modeled with a *cis* peptide, so again the *cis*-peptide is conserved even when the Pro residue is not.

As for the b_6f complexes, they seem to have *cis*-prolines at the beginning of helix C and E. There is no helix H, and the superimposed

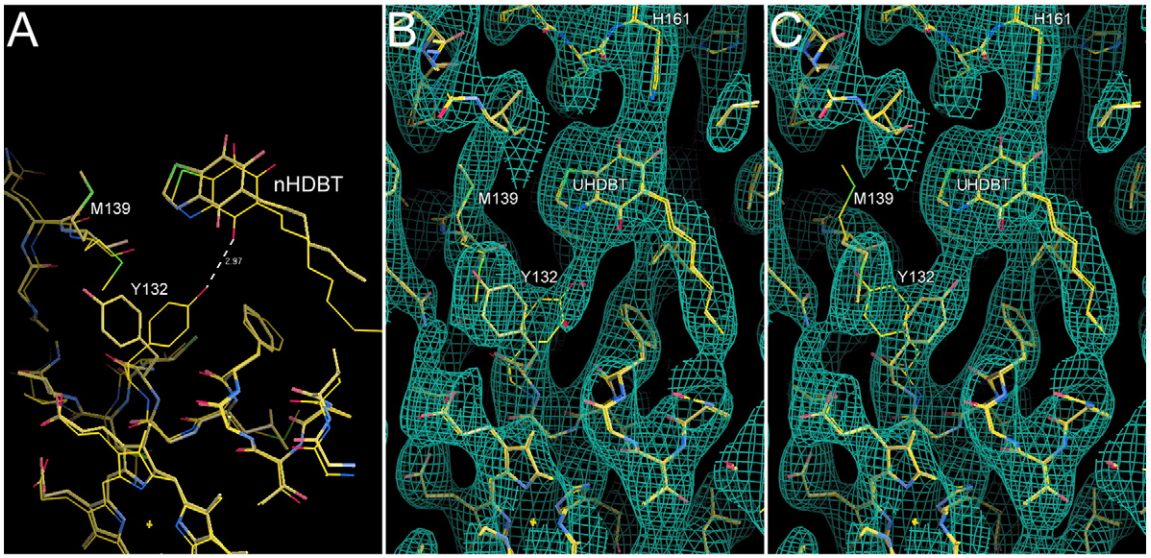

Fig. 7. Alternate conformations for Y132 and M139 in the presence of alkyl-HDBT? A. Superposition of structures 1p84 (thick bonds) and 1sqv (thin). B and C, Density maps using unpublished 3.26A data from chicken bc_1 crystal with UHDBT. Refined models starting with the conformation of 1p84 or 1sqv are shown in both. In B, the density is calculated using phases from the model based on 1p84 which is shown with thick sticks. In C, the model based on 1sqv was used for phases and that model is rendered with thick sticks. Figure made with O [88].

structures diverge at the end of helix G, so although a sequence-based alignment puts P150 of subunit IV near P347 of yeast cyt *b*, there is no structural reason to align them.

Superimposing the structure of yeast bc_1 complex and cyt b_6f from *Chlamydomonas*, yeast P109 aligns with P113 of b_6 and yeast S223 with P33 of subunit IV. Both were modeled with *cis* peptides in the *Chlamydomonas* structure 1Q90. They were modeled with conventional *trans* peptides in the structures from cyanobacteria, however examination of the electron density for 2E74 suggests that *cis* peptides would fit better here[5].

Why do *cis*-peptides occur at the beginning of helices? Pal and Chakrabarti [66] reported non-pro *cis* peptides to be over-represented at the N-termini of helices, in what Richardson and Richardson [67] have called the N-cap position, the residue at the start of the helix whose O receives an H-bond from the helix but N does not make one. The *cis*-peptides at these three positions of cyt *b* are overwhelmingly occupied by proline in the second position, but occurrence of non-pro *cis* peptides at two positions is striking given the rarity of these bonds (0.03%). Apparently whatever causes *cis*-peptides at N-termini of helices is powerful enough to maintain the *cis*-peptide even if the Pro residue is mutated to something else, resulting in over-representation of non-pro *cis* peptides while the greater number of *cis*-pro peptides at the N-cap position does not stand out among the even greater frequency of *cis*-pro at other positions (5.7% of x-Pro bonds are *cis* [66]).

Cis-peptides may serve as powerful helix-breakers to stop the growth of a helix at a particular point once it is nucleated. Proline itself being an tertiary amide is unable to donate an H-bond to the O of a preceding residue. However proline residues are frequently found in helices. Helix capping by cis-peptides may be important in the folding of proteins. Fig. 8 shows on the left the electron density for the *cis* peptide at Ser232 in yeast cyt b, and on the right the H-bonding pattern around this peptide, with a canonical α-helix superimposed for comparison (thin wires).

The residues around the N-terminal end of these three helices do not superimpose well, but the H-bonding pattern is somewhat similar around residues 223 and 347. That at 223 is shown in Fig. 8b. The carbonyl O of the second residue of the *cis*-peptide, ser223 in this case, points forward making an α-helical H-bond with the residue four ahead in the sequence. That of the first residue, His222, i.e. the O of the *cis* peptide, points backwards away from the helix, making it impossible for this peptide to take part in helical H-bonding. However the residue before that (221) points forward and may H-bond the residue 3, 4, or 5 ahead in sequence. For several residues prior to that there are no helical bonds.

Simply having a *cis* peptide does not force the carbonyl to point backwards, nor is a cis-peptide required for it to point backwards (in fact the deposited structure with trans peptide has the carbonyl correctly pointing backwards). However with a *trans* peptide the flip which allows helical bonding would be greatly preferred energetically, while having a *cis* peptide is not compatible with α-helical geometry. The resulting flipped peptide breaks the helical bonding, and although the residue before the *cis* pair makes a somewhat helical bond, the geometry of this turn of the helix is now so different that the helix cannot grow back any farther.

The standard program for classifying secondary structure, DSSP [68] assigns the helix start to the residue before the *cis*-dipeptide, 221 in this case. With that definition, the usually proline residue is not the Ncap but N2 residue. The arrangement around the *cis*-peptide at 108–109 is different, with the first residue of the helix being the one after Pro109; Pro109 not making a helical H-bond. i.e. instead of being a cap residue, the *cis*-pro is separated from the helix by one residue. Maybe the cis-peptides fix the ends of helices at an early stage in folding, but in the final structure they are displaced from the Ncap position.

Since Pro is not required to make the *cis*-peptide, there seems to be no way to use mutagenesis to probe the importance of these *cis*-peptides. However one might expect that one of the assembly factors being discovered for the bc_1 complex will be a peptidyl isomerase, and its deletion may lead to misfolding of cyt *b*.

5. What is the function of the Core proteins?

The two largest subunits of the mitochondrial bc_1 complex were originally termed "Core" proteins on the assumption that they would form the core of the complex. As it turns out they are peripheral both structurally (extra-membrane attachments on the matrix side) and functionally (not present in bacterial bc_1 or b_6f). The Core proteins are homologous to the β- and α-subunits of matrix processing peptidase

[5] Difference maps calculated from the deposited structure and data have positive peaks 5.9 and 6.5σ at the position where the carbonyl O of the first residue of the hypothetical *cis* peptide (A112 and B32) would be. Converting the peptide to *cis* and refining eliminates these difference densities. Further, The header of pdb file 2E74 flags a too-close contact between the carbonyl O of A112 and the Glu115 carboxylate of 1.99 Å, which is removed in the *cis* model.

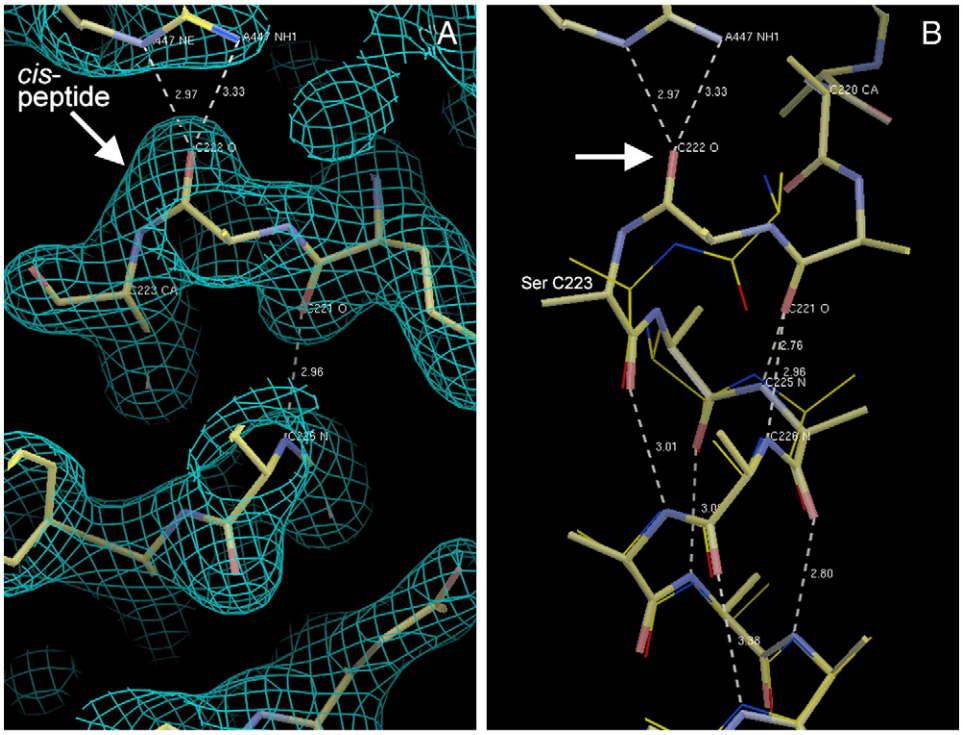

Fig. 8. The cis-peptide H222-S223 at the beginning of Helix E of cytochrome *b* in the yeast bc_1 complex. Left, atomic model with electron density, from structure 3cx5 after further refinement. The electron density is a 2mFo-DFc map from Phenix contoured at 1.5 σ. On the right is the same model with the side chains of the helix truncated to C^{β} for clarity. The arrow indicates the carbonyl O of His222 which due to the cis-peptide points away from the helix. At the top Arg447 of the Core 1 protein is visible H-bonding this atom, perhaps stabilizing the *cis*-peptide. For reference a canonical α-helix is superimposed (thin lines). In fungi other than *Saccharomycetae* and in most other eukaryotes and bacteria, the residue corresponding to Ser223 is a proline, and mutation to proline in yeast restores function to a complex with the gene for the core 2 protein deleted. Figure made with O [88].

(MPP), a metalloprotease responsible for removing leader sequences of imported proteins. In plants, the Core proteins are the MPP enzyme. In vertebrates and in yeast there are separate genes coding for Core proteins and MPP. Like MPP, the Core proteins consist of an α-β heterodimer of structurally related bowl-shaped subunits which come together to enclose an internal cavity, open to the outside through one gap, or "mouth", between the edges. The active site of MPP is within the internal cavity.

By sequence homology Core protein 1 corresponds to the catalytic β subunit of MPP, and Core protein 2 to the α subunit. The zinc binding motif of β-MPP is not conserved in vertebrate or yeast Core 1 (Fig. 9), and the X-ray structure of a bc_1 complex crystal soaked with zinc did not show any Zn binding in the Core proteins [69], suggesting it no longer has a proteolytic function. However there is circumstantial evidence for a proteolytic function in vertebrate mitochondria, in what appears to be an extreme case of product inhibition. MPP binds substrate peptides inside the cavity, with the scissile bond at the active site. In vertebrate bc_1 complexes, the signal peptide of the ISP is retained in the mature complex after cleavage, and is located within the cavity of the Core proteins. This suggests that the Core proteins may serve as processing peptidase for the bc_1 complex subunits, or at least for the ISP. In fact if the signal peptide is cleaved by soluble MPP, it is hard to imagine how or why it would subsequently be transferred to the interior of the Core proteins.

Furthermore the N-terminus of the mature ISP is on the outside of the Core proteins, near the edge of the mouth (Fig. 10). This suggests [9] that the Core proteins serve to cleave the signal peptide from the ISP after it is inserted into the complex, and what we observe in the crystal structure is the aftermath of the last, or only, proteolytic event of the Core proteins. We will examine the structure to see how consistent it is with this picture below.

```
S. cere βMPP    VKNNGTAHFLEHLAFKGTQNRPQQGIELEIENIGSHLNAYTSRENTVY→DVIIRESEEV
N.crassa C 1    DETNGTAHFLEHLAFKGTTKRTQQQLELEIENMGAHLNAYTSRENTVY→DVILRESEEV
beef core 1     EKNNGAGYFVEHLAFKGTKNRPGNALEKEVESMGAHLNAYSTREHTAY→DVILQELQEN
chick core 1    EKNNGAGYFVEHLAFKGTKKRPCAAFEKEVESMGAHFNGYTSREQTAF→GVILQELKEM
yeast core 1    PYNNGVSNLWKNIFLSKENS-------AVAAKEGLALSSNISRDFQSY→KSVLKQVQDF

N.crassa αMPP   DYVRGASHIMDRLAFKSTSTRTADEMLETVEKLGGNIQCASSRESMMY→MTAQYEVNEI
N.crassa C 2    L--PGLTVGLEEFAFKNTNKRTALRITRESELLGGQLQAYHTREAVVL→ENCIHEKQAK
S.cere αMPP     RNLKGCTHILDRLAFKSTEHVEGRAMAETLELLGGNYQCTSSRENLMY→LSAEYEIDEV
beef core 2     SNNLGTSHLLRLASSLTTKGASSFKITRGIEAVGGKLSVTSTRENMAY→PQLRIDKAVA
chick core 2    TANLGTAHLLRLASPLTTKGASSFRITRGIEAVGGSLSVYSTREKMTY→PQLKVDKAVA
yeast core 2    KD--GVAHLLNRFNFQNTNTRSALKLVRESELLGGTFKSTLDREYITL→PAARYDYAVA
```

Fig. 9. Alignment of Core and MPP proteins around Zn-binding site. The reverse Zinc motif "HxxEH … E" is underlined, and conserved residues of it are in bold. The complete motif is present here only in *S. cerevisiae* β-MPP and *N. crassa* Core 1; however the beef core 1, in which the first H has been mutated to Y, has been shown to have proteolytic activity, and mutation of that to S inactivates. Figure made with Clustalw at NPS@, PBIL [91].

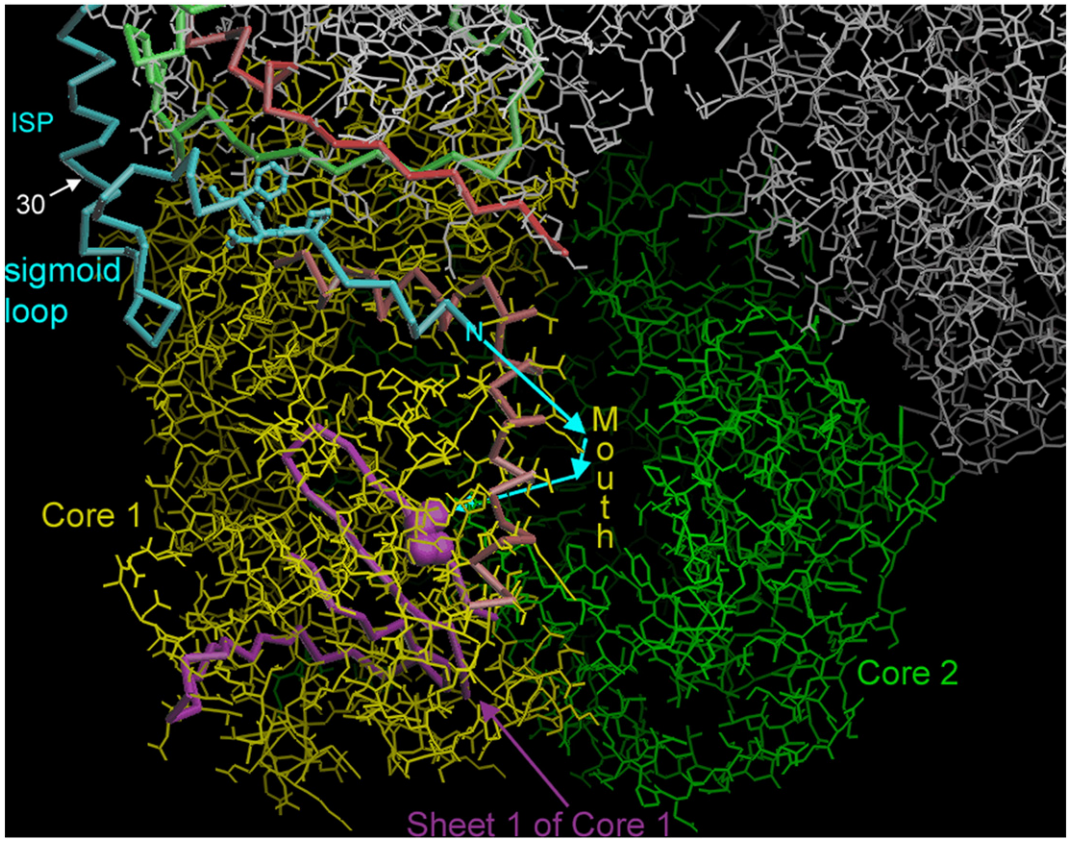

Fig. 10. N-terminus of the Rieske ISP in relation to the putative proteolytic site of core 1. The ISP is a cyan C^{α} trace. Peptides to be cut by MPP bind as an additional strand on the inside edge of sheet 1 of core 1, depicted in magenta. The rest of core 1 is yellow, core 2 is green. The bent brown helix is Helix D of core 1 which forms the lip of the mouth. A pathway from the N-terminus of the ISP to the proteolytic binding site is indicated by cyan arrows, and it is estimated that the ISP would reach there if the sigmoid loop straightened out. Residues 8PDF of the conserved motif are depicted on the ISP. P8 and F10 insert in the groove between side chains of β strands contributed by subunit 7 (green tube) and cyt c_1 (red tube). Figure made with O [88]. Stereo pairs (cross-eyed and wall-eyed) of this view are available in the supplemental materials.

In fact proteolytic processing activity has been demonstrated in the bovine bc_1 complex after detergent treatment [70], or from heterologously expressed Core proteins [71]. In the latter case no detergent treatment is required, but if the substrate is the ISP presequence then the activity is inhibited after a single turnover and can be reactivated by detergent treatment. This supports the conclusion that the requirement for detergent is to dissociate the product peptide.

Weiss and coworkers [72] used detergent and high salt to split the *Neurospora crassa* bc_1 complex into Core proteins, ISP, and a complex devoid of both. Activity could be reconstituted by adding both ISP and Core proteins, but not by ISP alone [73]. This would seem to imply a function beyond signal peptide processing, perhaps in re-insertion of the ISP (as described below, the mature N-terminus is associated with the Core proteins), or in maintaining the integrity of the structure to allow electron transport. Removal and reconstitution of the Core proteins apparently have not been reported in any other organism.

Another clue to the function of the Core proteins may be found in a yeast mutation that "obviates the need for Core protein 2" [74]. This mutation, S223P in cyt *b*, was originally isolated as a second-site revertant to a mutation resulting in truncation of Core 2, and it was shown that the cyt *b* mutant was still respiratory-competent with the Core 2 gene deleted entirely. Several factors make this mutation interesting: For one thing, there is a highly conserved proline at this position in the wild type of vertebrates, purple bacteria, and cyt b_6f subunit IV. Thus the mutation is restoring the residue that practically every other bc_1 complex has in the wild type. Secondly the peptide bond between P223 and the preceding residue is *cis* in the available structures: chicken, cow, *R. capsulatus* or *sphaeroides*, and b_6f. This could explain the highly conserved proline, as non-proline *cis* peptides are rather unstable. As described in the previous section, this is one of three *cis* peptides occurring at the start of transmembrane helices in cyt *b*, and they may play a role in folding; in defining the start of the helix, and although the Pro residue is not conserved in wild-type yeast, the peptide is still in a *cis* conformation.

But what has this got to do with the function of the Core 2 protein? This is not entirely clear, as Core 2 does not even make van-der-Waals contact with cyt *b*. However residue Arg447 in Core 1 protein makes a double H-bond to the carbonyl of residue 222, stabilizing the *cis* conformation of the 222–223 peptide. A highly speculative scenario is the following: If the *cis*-peptide is required for maintaining the proper fold of cyt *b*, perhaps the proline is stable in the *cis* form but serine will revert to *trans* if not stabilized by the H-bond between Arg447 and the carbonyl. Arg447 is in Core 1 not Core 2, but assuming the Core proteins form α-β heterodimers like MPP before binding the bc_1, then eliminating or truncating Core 2 would prevent heterodimer formation and Core I alone would probably not assemble into the complex. However this would not explain the need for Core proteins in other organisms, which have proline here in the wild type. And the H-bond with Arg447 is not special to yeast. This residue is highly conserved in Core 1 proteins, and makes the same H-bond in beef and chicken crystals.

The bc_1 complex was not isolated from the S223P mutant to see whether it contained any Core protein, for example a Core 1 homodimer, or a heterodimer with MPP providing a Core 2 replacement or the entire heterodimer. Perhaps the mutation S223P allows some such dimer to replace the Core proteins' function. Further investigation of this mutant, including attempts to isolate functional bc_1 from the Core 2 deletion and determine its subunit composition, would seem to be warranted.

Next we consider to what extent the arrangement of the ISP N-terminal region and the cleaved presequence with respect to the Core proteins in the mature complex is indicative of cleavage of the two apart as the last catalytic act of the Core proteins. First, does processing of the ISP occur before or after incorporation into the complex? The observation that the presequence is retained in the complex suggested that processing occurred after incorporation [75], but this is less compelling now that we know it is trapped inside the cavity of the Core proteins, at least if we accept they are the protease responsible for its cleavage. In yeast, a strong case was made that the second step of processing, by MIP, occurred after incorporation [76], but what about the MPP step, which is the only step in vertebrates?

Maturation of the ISP cluster in yeast requires subunit QCR9, and bc_1 isolated from QCR9 deletion strains by the lauryl maltoside method or digitonin extraction and BN PAGE do not contain the ISP [39,77], however the ISP is processed to maturity in the absence of QCR9 [77]. This would seem to imply that processing occurs, or at least can occur, before incorporation. However there is some evidence for incorporation in the absence of QCR9, in a detergent-labile, EPR-silent form [77].

If the Core proteins function like MPP, the pre-cleavage location of the scissile peptide in the active site can be accurately determined by superimposing yeast MPP X-ray structures [78] on the bovine Core proteins. Despite the amino acid differences, the backbones superimpose very well in the region of the active site. In the structure of the substrate complex of yeast MPP with Cox4 presequence (1HR8), the backbone N atom of the residue following the cleaved bond H-bonds to the carbonyl O of residue 101 of the catalytic β subunit, and the carbonyl O of the next to last residue before the cleaved bond binds to 103. This holds the peptide so the carbonyl O of the cleaved peptide bond is directed toward the Zn ion. Superimposing MPP on the bovine Core proteins, residues 101 and 103 correspond to A88 and A90 in Core 1. To reconstruct a pre-cleavage structure for the bovine ISP+Su9 precursor, we need to move residue 1 of the mature ISP to bond with residue 88, and next-to-last residue R77 of subunit 9 to bond with 90, of Core 1. If this can be done with relatively small movement of the termini of these proteins, leaving the ISP transmembrane helix in place and keeping the strand of subunit 9 attached to the scaffolding site in sheet 1 of Core 2, it supports the hypothesis that the existing condition arose by these termini relaxing to their current position after cleavage of the bond.

Chain-tracing of subunit 9, the leader peptide, is uncertain so the conclusion depends on which model you use. The possibilities will be considered in the next section. As for the mature ISP, the N-terminus is not very close to A88, however the first 24 residues, before the start of the transmembrane helix, are rather unstructured and trace a sigmoid path (Fig. 10), and it is not unreasonable to suppose they have drifted into this position after being released by cleavage.

The transmembrane helix of the ISP starts at residue 25 of the mature protein. Before there, going from the start of the transmembrane helix backwards toward the N-terminus, the ISP continues downward (in the orientation of Fig. 10) along the surface of Core 1, turns back upward and then downward again, with the N-terminus reaching nearly to Core 1 helix D which forms an edge of the mouth opening into the internal cavity. Assuming everything before the transmembrane helix may have moved after release by cleavage, we can ask if 24 residues could stretch from the active site at residue A88 in the Core 1 protein, out through the mouth, around helix D to the beginning of the TM helix at 25. The path from the current position of the N-terminus to the active site is indicated by blue arrows in Fig. 10. In the most extended β form, a polypeptide can reach about 3.3 Å per residue, so the 24 residues could reach at most 79 Å.

Residue 25 of the ISP is close to Core 1, but it is on the outside of this bowl-shaped subunit. Assuming the peptide would have to enter the central cavity through the mouth rather than penetrating the wall of the bowl, it must go around Helix D of Core 1. Taking a path by residue A139 in helix D as the shortest distance, the sum of the distances from ISP:25 to A139 and from A139 to the active site at A88, plus another 15 Å to go around A139 with a 5 Å radius gives 72 Å. Thus it would be feasible to reach, but with little slack to spare. Of course in the pre-protein there would be an additional 78 residues to diffuse into the cavity, binding initially near the pre-protein N-terminus, and then by attaching successive segments to the binding scaffold, draw the protein in up to the cleavage site. It is tempting to propose that this process of the Core protein drawing the presequence in until the scissile bond is at the active site, plays a role in positioning the ISP within the complex. However it must be remembered that mature ISP can be used to reconstitute the bc_1 complex, as has been shown in many labs by many different procedures [72,79–83], so the presequence is not required for positioning. In these experiments the ISP does in fact go back in the correct position rather than adsorbing its TMH to the surface in a position that allows function, since reconstitution is inhibited by excess of the TMH segment [82].

What about the yeast ISP? The ISP of *S. cerevisiae* has a 30-residue leader peptide which is removed in two steps — the first 22 residues (underlined in Fig. 11) by MPP or Core protein, and the final octapeptide (double-underlined) by MIP [84]. This leaves the N-terminus of the mature ISP shorter than that of the bovine protein by 10 residues, measured from superimposing residues in the TMH. The difference in length is made up in the sigmoid loop (9 residue deletion in Fig. 11), and the N-terminus of the mature ISP is in nearly the same position as that of the vertebrate protein, near the mouth of the Core protein heterodimer. The backbones of the two proteins are nearly identical for residues 7–14 of the vertebrate ISP and 6–13 of the yeast protein (36–43 of the pre-protein), where the protein passes over β-sheet 2 of Core 1. Using this structural alignment to guide sequence alignment (Fig. 11) shows a motif (R/K)xP(D/N)FxxY (boxed region in Fig. 11) in this accurately superimposing region, and the highly conserved P and F are facing the groove in β-sheet 2 between strands contributed by cyt c_1 and subunit 7 (QCR8). Presumably this is a tight, specific binding interaction which serves as an anchor to fix the position of the N-terminal segment. Between this and the transmembrane helix is the sigmoid loop, which is shorter by 9 residues in yeast (5 residues 46 to 50 replace 14 residues 17 to 30, using the pre-protein sequence for yeast and the mature sequence for vertebrates). From there on the sequence numbers have a constant offset of 20, leading to the confusing situation that cluster-binding histidine 161 of yeast corresponds to cluster-binding histidine 141 of vertebrates.

What does this imply for the possibility of the yeast protein being processed by the Cores after insertion to its final place? Although the mature N-terminus is 10 residues shorter, the Core proteins would be cutting at the MPP site which is distal to the octapeptide, so only two residues shorter than the vertebrate cutting site. And this could be made up by the fact that the yeast protein doesn't join the vertebrate for the first, kinked turn of the transmembrane helix at residue 25, but rather at 30 where the main helix begins. So it would be possible for the scissile bond to reach the active site in the Core proteins, and the length of polypeptide from there to the transmembrane helix would be about the same as in vertebrates, despite the facts that the conserved anchor segment is displaced nine residues relative to that of vertebrates and that the MIP removes an additional eight residues afterwards.

Although the cleaved presequence of vertebrates remains firmly bound in the interior of the Core proteins, the shorter presequence of yeast apparently does not, and in both the N-termini of the mature ISPs do not. As described in the next section, the tight binding of the vertebrate presequence is not at the cutting site but at the homologous site in Core 2, one of the "scaffolding" binding sites. It involves adding a β− strand to the inner edge of sheet 1 of Core 2. Again looking at the reactant complex of the yeast MPP with Cox4, the stretch containing the scissile bond binds in the same way on Core 1 but with a less extensive sheet involving only three H-bonds. After cleavage the two ends would

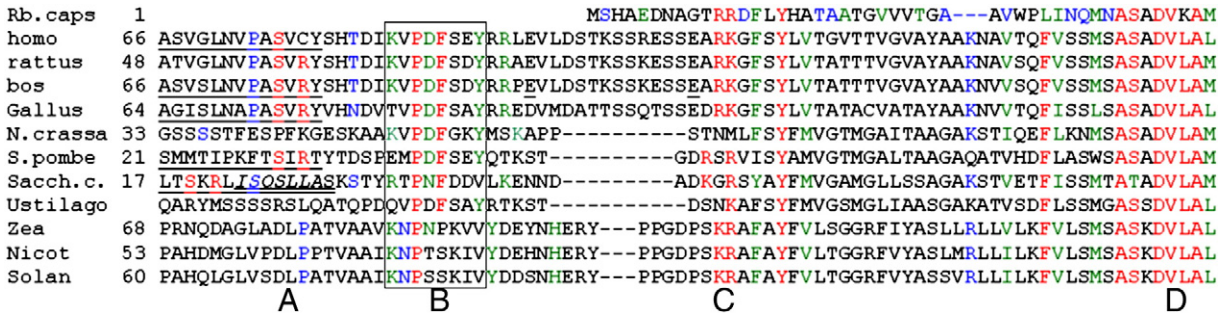

Fig. 11. Sequence alignment of N-terminal region of Rieske ISP precursor proteins. Underlined regions indicate signal peptide sequence removed by MPP. Doubly underlined octapeptide of *S. cerevisiae* is the region removed by MIP in a second processing step. Higlighted SxR sequence A includes the R at -2 to the MPP cleaveage. Boxed region B has the KxPDFxxY motif which in vertebrates and yeast, lies on the groove betweeen strands contributed by cyt c_1 and subunit 7 (QCR8) to β-sheet 2 of core protein 1. Twin basic residues C anchor the start of the transmembrane helix at the membrane interface. Highly conserved region D at the far right is the "neck" region including the helix which partially unwinds when the ISP is in the b position. Figure made with Clustalw at NPS@, PBIL [91].

each be retained by only one or two bonds, so they would dissociate. The Cox4 presequence has only 17 residues and does not interact with the binding site in Core 2 the way the vertebrate ISP presequence does. The segment cleaved by MPP from the yeast ISP is only slightly longer, at 22 residues, and may also not make this interaction, accounting for its easy release after cleavage.

Why should the presequence be retained? If the Core proteins are involved in recruiting the ISP to the complex, then the idea [76] that having the presequence bound would prevent those complexes that already have ISP from recruiting another, makes sense. Or perhaps it is just optimizing substrate binding affinity. Normal enzymes must balance substrate affinity with the need to dissociate product. Unless the ISP turns over faster than the rest of the complex and needs to be replaced periodically, there is no need for the processing peptidase to catalyze another cleavage, so no limit to how tightly the presequence could be bound.

Of course this is all speculation and does not answer the question of whether the Core proteins function as processing proteases. We think that the idea is plausible enough to stimulate someone to find a definitive answer. In the case of yeast this could be as simple as looking for Core 1 mutants that do not process the ISP, starting by mutating what is left of the Zn-binding site. In the case of the bovine Core 2 it was shown that mutating the Tyr71 to Thr completely abolishes processing activity. Perhaps the same thing could be done with mammalian cells in tissue culture, transfecting with mutant Core proteins and knocking down the endogenous protein. It has been shown in yeast that processing by MIP to remove the octapeptide is not required for function [85]. If the Core proteins are responsible for the MPP cleavage, a Core mutant might assemble a functional bc_1 complex with the unprocessed N-terminus of the ISP bound to the active site inside the Core proteins.

6. What is the correct tracing for subunit 9 in the vertebrate bc_1 complex, and why is it retained in the mature bc_1 complex?

Why is the leader sequence of the ISP retained in the mature complex, and what is the correct tracing in the structures?

As described in the previous section, the vertebrates Rieske ISP are synthesized with a rather long (78 residues in beef) signal peptide which directs its import into the mitochondria. The signal peptide is cleaved off at some point during import and assembly, but surprisingly it is found in the mature complex as subunit 9. There are several strands of polypeptide within the internal cavity of the Core proteins which presumably belong to subunit 9 since all the other subunits have been accounted for, but they are not well ordered except for a short stretch, and the amino acids are not distinctive enough to allow positive identification from low resolution structures. Since the leader sequence is apparently not retained in fungi, plants, or protozoans; and of course does not exist in prokaryotes; it presumably does not play any important role in the basic functions of electron transport and proton pumping.

However the structure of subunit 9 may hold a key to the function of the Core proteins. Presence of the leader sequence of the ISP inside the Core proteins suggests the possibility that leader sequence is cleaved by the Core proteins and never dissociates afterwards [9]. We would like to know how consistent the arrangement of the leader sequence in the mature complex is with that scenario.

The various structures coming out in 1997–1998 all included bits of subunit 9 in the cavity of the Core proteins, but they were quite different. The models have been modified some in later structures, but a consensus has not been reached. Fig. 12A illustrates the models of the ISP in structures 1be3 [9], 1ppj [10], and 2fyu [15]. Fig. 12b shows schematics of the path through the density, which is apparently similar in all the structures, and details of the ways in which the chain has been traced. One of the challenges is that the density seems to come together at a number of nodes where three strands of density converge. This could be due to multiple arrangements in different unit cells being superimposed in the electron density, but it could also be due to confusion of main chain vs side chain and close connection of the side chain to other density.

There is one stretch of 5 residues (labeled *a* in Fig. 12) which is well ordered due to binding as an additional strand to β-sheet 1 of Core protein 2. This is one of the four internal sheet edges that have been identified as a "binding scaffold" for substrate peptides [78]. There is density that can be modeled as a second strand (*b*) parallel to that. Then there are stretches of density leading from near either end of the β sheet, across the cavity, to the mouth. One of these, labeled *c*, runs along sheet 2 of Core 2 near the internal edge, but not as an additional strand of the sheet. At the end of **c** near the mouth, there is a helix or zigzag. The other (*d*) is not modeled in 1be3 but is present in other structures from beef and chicken. Finally there is a short stretch (*e*) near the beginning of strand a that has been modeled as the N-terminus in 2fyu.

The well-ordered stretch *a* is at least traced in the same direction in all the models, antiparallel, as is the rest of the sheet, bonding to residues 100 to 96 in strand D[6] of sheet 1 of the Core 2 protein. These 5 residues were modeled as 67SVSLN in 1be3, 66ASVSL in 1ppj, and 13PVLSA in 2fyu.

From the density in 1ppj and related crystals, the first four of these residues and the preceding one all have small side chains, so the Leu residues in the 1be3 and 2fyu models cannot be well accommodated. In particular L70 of 1be3 is on a residue (position 4 of the 5) which appears to be glycine in the density of 1ppj. In 1ppj the sequence is as in 1be3 but translated ahead by 1. This puts the big leucine 70 in density, but V68 and S69 appear too big for their density.

In fact there are only two stretches in the bovine leader peptide that have 5 consecutive small residues: 21GVAGA and 65VASVS. If

[6] Secondary structure elements of the core proteins are defined in ref [7].

proline is considered small, there is also 32AAVPATS, but proline would probably be recognizable. In any case, we have not found any stretch of sequence that fits this well. It is possible that binding is promiscuous with respect to register, in which case a single large residue could be present at low occupancy at several places and not visible at any.

In structures 1be3 and 1ppj, strand *a* is preceded by the stretch we have labeled *c*. The connection is different, with the main chain of 1be3 passing through density which is modeled as Arg62 side chain in 1ppj before entering strand *a*. On the other hand 2fyu connects appendix *e* to the beginning of *a*, and takes the end of *e* as the N-terminus. Stretch *e* is not modeled in any other published crystal forms. This area is quite noisy in our chicken or beef crystals. However on superimposing 2fyu we found that the "noise" fits the first four residues MLSV extremely well, including the acetyl group on the N-terminal methionine; and the next several residues reasonably well. And this can be traced on into strand *a* as in 2fyu, with fair density for P10, although it puts F11, P13 and L15 in residues that seem to have smaller side chains.

After the well-ordered β strand *a*, most models have the peptide turning back on itself to make a second β strand in the sheet, but this is not as well ordered. In the model of 1be3 this leads to the C-terminus, but density for the last two residues (Arg Tyr) is not good in 1ppj, and could be modeled as well by further extension of the peptide chain into a node where other density connects. In the tetragonal beef crystal 2fyu, the end of b connects to c. Alternatively, it can be reasonably be modeled (in 1ppj) as connecting to the start of segment a at one of two places indicated in scheme 5 or 6 of Fig. 12B.

Stretch c has been modeled in opposite directions, going toward the β strand in 1be3 and 1ppj, and away from it in 2fyu. Stretch c has a 2-turn helix in 2fyu, or one turn of helix and a zigzag in 1ppj, on the end near the mouth. Using the aRP/WARP autobuilding program [86] as a bias remover (iterative refinement as free atoms, adding new atoms, and chain-building from the atoms) stretches *c*, *a*, and *b* were preserved in the order of 1ppj in most cases, however on one occasion *c* was reversed. Now with a further refined version of 1ppj, and omitting all of subunit 9 from both monomers to completely avoid bias, aRP/WARP builds only three residues of *c*, in the helical turn. These are going in the direction of 1be3 and 1ppj, opposite 2fyu. With the model of 1be3 there are numerous long side-chains in this region, and the fit is pretty good but there are enough poor fits to raise some doubts. There is good density for Cys51 with its heavy sulfur atom. Seeing the anomalous signal of sulfur would be a good way to confirm this model, but our collection wavelength is too short and our accuracy too low to reliably locate the sulfur atoms in Bijvoet difference maps from any of our data.

Density at the beginning of b is also not good, auto-tracing starting with phases from a model with subunit 9 chains removed only built a tripeptide in the middle of b with no connection at the beginning as is made in all three structures. By making a main-chain/side-chain switch at the junction of a, b, and d; stretch a can be built continuing into d with a good fit to the density, as in schemes 5 and 6. In fact this is what aRP/WARP builds in the recent experiment mentioned above. It is also building a tripeptide in b, well positioned as another strand of the β sheet. However it has nowhere to go since it leads into c, a, and e. Stretches c and e are both coming toward it, unless in fact c is reversed as in 2fyu. It could turn into a as in scheme 6. Scheme 6 is meant to imply the N-terminus has two conformations — one in appendix e and the other folded over into second β strand b, both feeding into a. However a good model can be made with c leading into a as in 1be3, and this is what aRP/WARP is building with the current starting phases. So we have possibility of b, c, or e running into the well-ordered strand a. They could all do, as alternate conformations, but that would mean the occupancy of each is low.

How do these models fit with the idea that subunit 9 is left where it was bound when it was cleaved from the N-terminus of the ISP? None of the models have it binding to sheet 1 of Core 1 where the scissile bond-containing segment binds, but as explained in the previous section that binding is not extensive and would be expected to dissociate upon cleavage. What is most likely to be left over from pre-cleavage substrate binding is segment *a* on sheet 1 of Core 2,

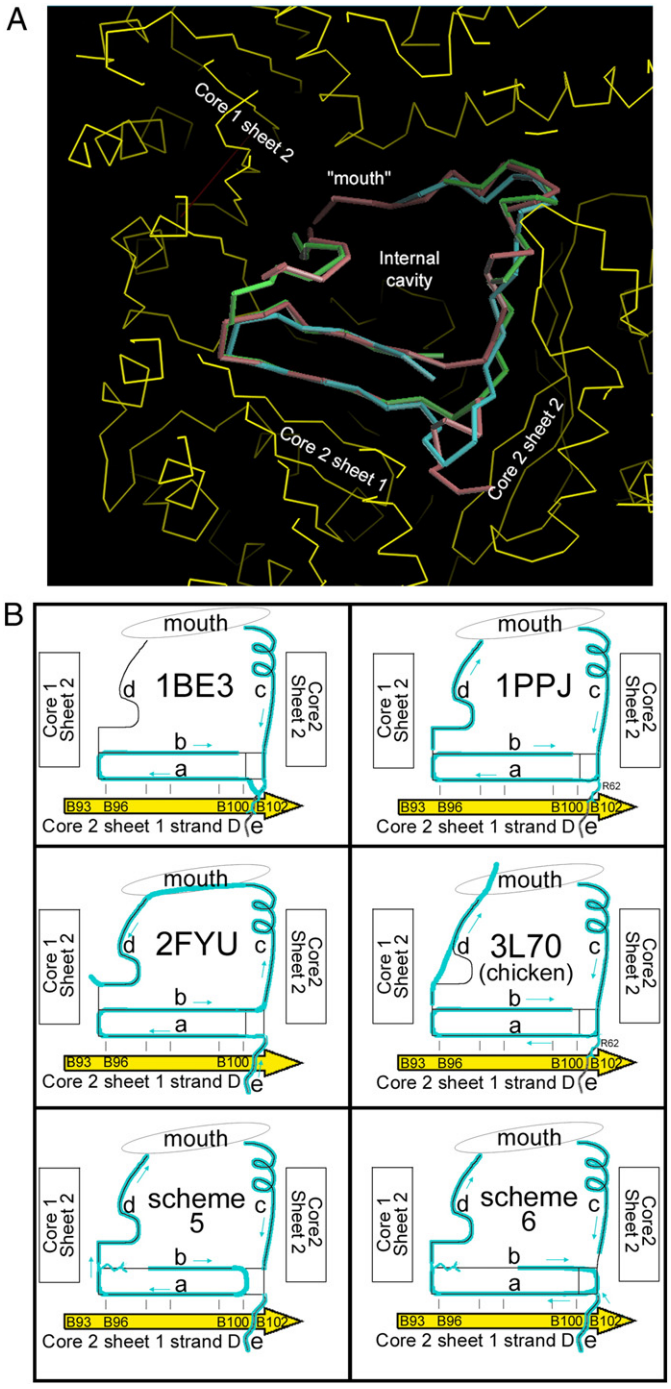

Fig. 12. Comparing subunit 9 as modeled in different structures. Above. superposition of subunit 9 from bovine structures 1be3 (blue), 1ppj (green), and 2fyu (brown). Below, schematic diagrams showing how those structures as well as 3L70 (chicken) and two unpublished schemes mentioned in the text, trace subunit 9. The yellow arrow represents strand D of subunit 2, on which subunit 9 adds an additional sheet. Upper figure made with O [88].

part of the binding scaffold. The last residue involved in this b-strand, the one bonded to residue 96 of Core 2, is 71 in 1be3 and 17 in 2fyu. From C^{α} of this residue, there is a straight path of 32 Å across the internal cavity to residue 90 in Core 1 where the residue 77, that is −2 from the scissile bond, would bind (see previous section). This is too short to be reached with the models of 1be3 or 1ppj without some unzipping of segment *a* from sheet 1 but compatible with 2fyu in which the N-terminus binds to sheet 1 of core 2.

7. Are the cyt b_L hemes promiscuously oriented? And what is the chirality of Met S^{δ} that ligates heme c_1?

Heme *b*, or iron protoporphyrin IX, is a pseudosymmetric molecule, with everything symmetric about a dividing line (mirror plane) between the A and B rings on one side and C and D rings on the other, except that the methyl and vinyl substituents on rings B and C are switched. Since this depends on the absence or presence of a single carbon atom at the four places, the orientation is not always clear in low resolution structures.

All of the yeast and chicken structures, and the orthorhombic beef structures like 1ppj, have the hemes oriented consistently, although this may be because each structure was solved using the best available previous structure. Structures from the tetragonal beef crystals have heme b_H oriented as in the yeast and chicken structures, but different structures have different orientations for b_L. Interestingly, the first C^{α}-only structure 1qcr and the highest-resolution most recent structure 2fyu both have heme b_L oriented in the opposite direction to the yeast and chicken structures.

Looking at our highest resolution bovine structure 1ppj, the density seems to support our structure pretty well, but this is in part due to model bias. As a more rigorous test, the C^{β} atoms were removed from the vinyl groups leaving effectively methyls in all four places, and this structure was refined to convergence. A difference map calculated using phases from this model showed positive density peaks of about 0.3 $e^{-}/Å^3$ at the original vinyl positions (Fig. 13). The highest difference density around the other two substituents was below 0.1 $e^{-}/Å^3$, which is around the noise level of the map. A similar situation was observed in the other monomer.

This supports the idea that heme b_L has a preferred orientation, specifically when viewed from His84 (83 beef, 82 yeast; from helix B side) the rings A B, C, D or I, II, III, IV go around in a clockwise direction, as in chicken and yeast structures, and bovine structure 1ppj. However it is much less clear in a number of other structures. It might be useful to compare the two orientations by calculating binding energy with a docking program, to see if one orientation gives better contacts.

Another question regards the chirality of the S atom of the methionine residue that coordinates heme c_1. The sulfur atom has tetrahedral geometry (sp^3 hybridization) and two lone pairs of electrons. When one of these lone pairs coordinates the iron, it generates a chiral center at S, the chirality of which depends on which lone pair is involved [87]. Visually this manifests itself in the direction that the C^{ε} methyl group points. If the smallest angle from C^{γ} to C^{ε} about S^{δ} (viewed from the Met side, perpendicular to the plane of the heme) is going clockwise from C^{γ} to C^{ε}, the chirality is **S**. If counterclockwise, it is **R**. mitochondrial cyt *c* and alphaproteobacterial cyt c_2 have **R** chirality. It is now pretty clear that it is **S** in cyt c_1, based on most recent and highest resolution structures from yeast (3cx5), beef (1ppj, 2fyu), or chicken (3L70). However some of the pioneering structures (e.g. 1be3, 1L0n) had it the other way, perhaps due to using cyt *c* as a model and for topology and parameters.

8. Conclusions

Synthesizing the crystallographic results for cytochrome bc_1 from a number of different crystal forms in the presence of various inhibitors presents a more complete picture of the structure than any one crystal form could have provided, and also provides warning of possible uncertainty when the structures disagree. This approach would be even more powerful if diffraction data were made available for all of the structures.

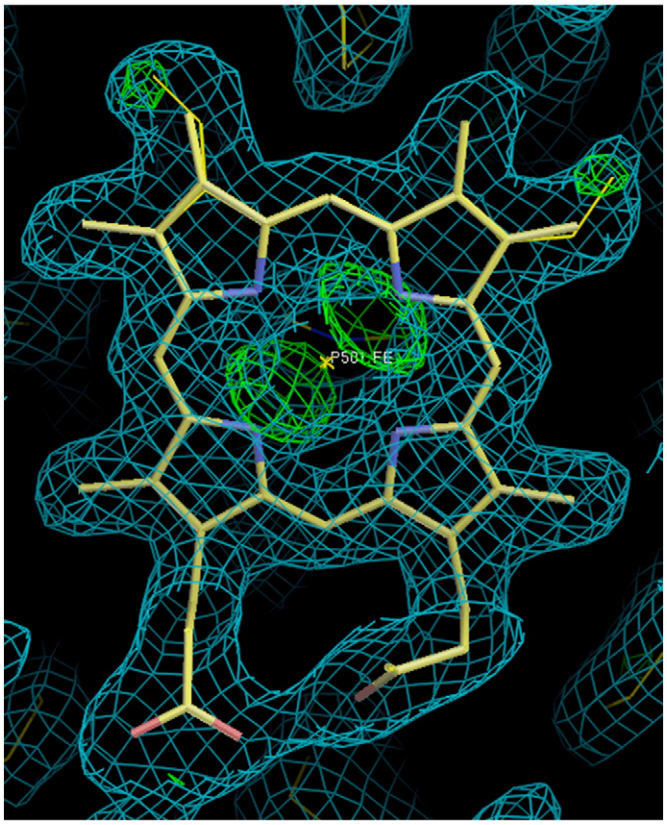

Fig. 13. Determining heme orientation from an omit map. Structure 1ppj after further refinement was used to look for asymmetry in the b_L heme which would imply specific orientation. The C^{β} atoms were removed from both vinyl groups. After further refinement to convergence, maps (2Fo − Fc and Fo − Fc) were calculated. The 2Fo − Fc map contoured at 0.3 $e^{-}/Å^3$ is shown in blue, and the difference map contoured at 0.27 $e^{-}/Å^3$ is green. The truncated heme used for refinement and phasing is shown as thick bonds. while the original refined heme is shown with thin bonds to show where the atoms were removed. Points of positive difference density show that something is missing where the C^{β} atoms were removed, suggesting that the original orientation was correct. The large positive difference density symmetrically located about the heme iron probably results from aniosotropic motion of this electron-dense atom. Figure made with O [88].

Acknowledgements

Drs. Tom Fox and Xinjie Chen provided valuable advice and assistance in constructing the cytochrome b mutants in yeast. We are thankful for the constructive comments of a diligent anonymous reviewer. During the time this review was written E.A.B. and L-S.H. were supported by new faculty startup funds from State University of New York (SUNY). H.DB. was supported by a graduate student line from the SUNY Upstate Medical University College of Graduate Studies.

Appendix A. Supplementary data

Supplementary data to this article can be found online at http://dx.doi.org/10.1016/j.bbabio.2013.04.006.

References

[1] D.H. Deul, M.B. Thorn, Effects of 2,3-dimercaptopropanol and antimycin on absorption spectra of heart-muscle preparations, Biochim. Biophys. Acta 59 (1962) 426–436.

[2] G. von Jagow, W.D. Engel, Complete inhibition of electron transfer from ubiquinol to cytochrome b by the combined action of antimycin and myxothiazol, FEBS Lett. 136 (1981) 19–24.
[3] A. Crofts, B. Hacker, B. Barquera, C.H. Yun, R. Gennis, Structure and function of the bc-complex of *Rhodobacter sphaeroides*, Biochim. Biophys. Acta 1101 (1992) 162–165.
[4] M. Degli Esposti, S. De Vries, M. Crimi, A. Ghelli, T. Patarnello, A. Meyer, Mitochondrial cytochrome b: evolution and structure of the protein, Biochim. Biophys. Acta 1143 (1993) 243–271.
[5] W.S. Kunz, A. Konstantinov, Cytochrome b reduction by hexaammineruthenium in mitochondria and submitochondrial particles. Evidence for heme b-562 localization at the M-side of the mitochondrial membrane, FEBS Lett. 175 (1984) 100–104.
[6] S. Hong, N. Ugulava, M. Guergova-Kuras, A.R. Crofts, The energy landscape for ubihydroquinone oxidation at the Q(o) site of the bc(1) complex in *Rhodobacter sphaeroides*, J. Biol. Chem. 274 (1999) 33931–33944.
[7] D. Xia, C.A. Yu, H. Kim, J.Z. Xia, A.M. Kachurin, L. Zhang, L. Yu, J. Deisenhofer, Crystal structure of the cytochrome bc1 complex from bovine heart mitochondria, Science 277 (1997) 60–66.
[8] Z. Zhang, L. Huang, V.M. Shulmeister, Y.I. Chi, K.K. Kim, L.W. Hung, A.R. Crofts, E.A. Berry, S.H. Kim, Electron transfer by domain movement in cytochrome bc1, Nature 392 (1998) 677–684.
[9] S. Iwata, J.W. Lee, K. Okada, J.K. Lee, M. Iwata, B. Rasmussen, T.A. Link, S. Ramaswamy, B.K. Jap, Complete structure of the 11-subunit bovine mitochondrial cytochrome bc1 complex, Science 281 (1998) 64–71.
[10] L.S. Huang, D. Cobessi, E.Y. Tung, E.A. Berry, Binding of the respiratory chain inhibitor antimycin to the mitochondrial bc(1) complex: a new crystal structure reveals an altered intramolecular hydrogen-bonding pattern, J. Mol. Biol. 351 (2005) 573–597.
[11] C. Hunte, J. Koepke, C. Lange, T. Rossmanith, H. Michel, Structure at 2.3 A resolution of the cytochrome bc(1) complex from the yeast *Saccharomyces cerevisiae* co-crystallized with an antibody Fv fragment, Structure, Fold. Des. 8 (2000) 669–684.
[12] C. Lange, C. Hunte, Crystal structure of the yeast cytochrome bc1 complex with its bound substrate cytochrome c, Proc. Natl. Acad. Sci. U. S. A. 99 (2002) 2800–2805.
[13] S.R. Solmaz, C. Hunte, Structure of complex III with bound cytochrome c in reduced state and definition of a minimal core interface for electron transfer, J. Biol. Chem. 283 (2008) 17542–17549.
[14] E.A. Berry, L.-S. Huang, L.K. Saechao, N.G. Pon, M. Valkova-Valchanova, F. Daldal, X-ray structure of *Rhodobacter capsulatus* cytochrome bc1: comparison with its mitochondrial and chloroplast counterparts, Photosynth. Res. 81 (2004) 251–275.
[15] L. Esser, X. Gong, S. Yang, L. Yu, C.A. Yu, D. Xia, Surface-modulated motion switch: capture and release of iron–sulfur protein in the cytochrome bc1 complex, Proc. Natl. Acad. Sci. U. S. A. 103 (2006) 13045–13050.
[16] L. Esser, M. Elberry, F. Zhou, C.A. Yu, L. Yu, D. Xia, Inhibitor-complexed structures of the cytochrome bc1 from the photosynthetic bacterium *Rhodobacter sphaeroides*, J. Biol. Chem. 283 (2008) 2846–2857.
[17] T. Kleinschroth, M. Castellani, C.H. Trinh, N. Morgner, B. Brutschy, B. Ludwig, C. Hunte, X-ray structure of the dimeric cytochrome bc(1) complex from the soil bacterium *Paracoccus denitrificans* at 2.7-A resolution, Biochim. Biophys. Acta 1807 (2011) 1606–1615.
[18] D. Stroebel, Y. Choquet, J.L. Popot, D. Picot, An atypical haem in the cytochrome b(6)f complex, Nature 426 (2003) 413–418.
[19] E. Yamashita, H. Zhang, W.A. Cramer, Structure of the cytochrome b6f complex: quinone analogue inhibitors as ligands of heme cn, J. Mol. Biol. 370 (2007) 39–52.
[20] C. Hunte, A. Kant, Crystallization of membrane proteins with the help of antibody fragments, in: C. Hunte, H. Schägger, G. von Jagow (Eds.), Membrane Protein Purification and Crystallization: a practical guide, Academic Press, 2001.
[21] A. Musatov, N.C. Robinson, Detergent-solubilized monomeric and dimeric cytochrome bc1 isolated from bovine heart, Biochemistry 33 (1994) 13005–13012.
[22] R.P. Joosten, K. Joosten, G.N. Murshudov, A. Perrakis, PDB_REDO: constructive validation, more than just looking for errors, Acta Crystallogr. D Biol. Crystallogr. 68 (2012) 484–496.
[23] A.R. Crofts, M. Guergova-Kuras, L. Huang, R. Kuras, Z. Zhang, E.A. Berry, Mechanism of ubiquinol oxidation by the bc(1) complex: role of the iron sulfur protein and its mobility, Biochemistry 38 (1999) 15791–15806.
[24] E.A. Berry, L.S. Huang, Conformationally linked interaction in the cytochrome bc(1) complex between inhibitors of the Q(o) site and the Rieske iron–sulfur protein, Biochim. Biophys. Acta 1807 (2011) 1349–1363.
[25] H. Kim, D. Xia, C.A. Yu, J.Z. Xia, A.M. Kachurin, L. Zhang, L. Yu, J. Deisenhofer, Inhibitor binding changes domain mobility in the iron–sulfur protein of the mitochondrial bc1 complex from bovine heart, Proc. Natl. Acad. Sci. U. S. A. 95 (1998) 8026–8033.
[26] L. Esser, B. Quinn, Y.F. Li, M. Zhang, M. Elberry, L. Yu, C.A. Yu, D. Xia, Crystallographic studies of quinol oxidation site inhibitors: a modified classification of inhibitors for the cytochrome bc(1) complex, J. Mol. Biol. 341 (2004) 281–302.
[27] U. Brandt, The chemistry and mechanics of ubihydroquinone oxidation at center P (Qo) of the cytochrome bc1 complex, Biochim. Biophys. Acta 1365 (1998) 261–268.
[28] A.R. Crofts, S. Hong, Z. Zhang, E.A. Berry, Physicochemical aspects of the movement of the Rieske iron sulfur protein during quinol oxidation by the bc1 complex from mitochondria and photosynthetic bacteria, Biochemistry 38 (1999) 15827–15839.
[29] X. Gao, X. Wen, C. Yu, L. Esser, S. Tsao, B. Quinn, L. Zhang, L. Yu, D. Xia, The crystal structure of mitochondrial cytochrome bc1 in complex with famoxadone: the role of aromatic-aromatic interaction in inhibition, Biochemistry 41 (2002) 11692–11702.
[30] S. Rajagukguk, S. Yang, C.A. Yu, L. Yu, B. Durham, F. Millett, Effect of mutations in the cytochrome b ef loop on the electron-transfer reactions of the Rieske iron–sulfur protein in the cytochrome bc1 complex, Biochemistry 46 (2007) 1791–1798.
[31] M.C. Lawrence, P.M. Colman, Shape complementarity at protein/protein interfaces, J. Mol. Biol. 234 (1993) 946–950.
[32] E.A. Berry, L.S. Huang, Z. Zhang, S.H. Kim, Structure of the avian mitochondrial cytochrome bc1 complex, J. Bioenerg. Biomembr. 31 (1999) 177–190.
[33] H.W. Ma, S. Yang, L. Yu, C.A. Yu, Formation of engineered intersubunit disulfide bond in cytochrome bc1 complex disrupts electron transfer activity in the complex, Biochim. Biophys. Acta 1777 (2008) 317–326.
[34] G. von Jagow, H. Schagger, W.D. Engel, P. Riccio, H.J. Kolb, M. Klingenberg, Complex III from beef heart: isolation by hydroxyapatite chromatography in Triton X-100 and characterization, Methods Enzymol. 53 (1978) 92–98.
[35] U. Brandt, H. Schagger, G. von Jagow, Characterisation of binding of the methoxyacrylate inhibitors to mitochondrial cytochrome c reductase, Eur. J. Biochem. 173 (1988) 499–506.
[36] U. Brandt, U. Haase, H. Schagger, G. von Jagow, Significance of the "Rieske" iron–sulfur protein for formation and function of the ubiquinol-oxidation pocket of mitochondrial cytochrome c reductase (bc1 complex), J. Biol. Chem. 266 (1991) 19958–19964.
[37] E. Davidson, T. Ohnishi, M. Tokito, F. Daldal, *Rhodobacter capsulatus* mutants lacking the Rieske FeS protein form a stable cytochrome bc1 subcomplex with an intact quinone reduction site, Biochemistry 31 (1992) 3351–3358.
[38] M.B. Valkova-Valchanova, A.S. Saribas, B.R. Gibney, P.L. Dutton, F. Daldal, Isolation and characterization of a two-subunit cytochrome b-c1 subcomplex from *Rhodobacter capsulatus* and reconstitution of its ubihydroquinone oxidation (Qo) site with purified Fe–S protein subunit, Biochemistry 37 (1998) 16242–16251.
[39] V. Zara, L. Conte, B.L. Trumpower, Evidence that the assembly of the yeast cytochrome bc1 complex involves the formation of a large core structure in the inner mitochondrial membrane, FEBS J. 276 (2009) 1900–1914.
[40] L. Conte, B.L. Trumpower, V. Zara, Bcs1p can rescue a large and productive cytochrome bc(1) complex assembly intermediate in the inner membrane of yeast mitochondria, Biochim. Biophys. Acta 1813 (2010) 91–101.
[41] D.J. Kolling, J.S. Brunzelle, S. Lhee, A.R. Crofts, S.K. Nair, Atomic resolution structures of rieske iron–sulfur protein: role of hydrogen bonds in tuning the redox potential of iron–sulfur clusters, Structure 15 (2007) 29–38.
[42] G. von Jagow, T. Ohnishi, The chromone inhibitor stigmatellin–binding to the ubiquinol oxidation center at the C-side of the mitochondrial membrane, FEBS Lett. 185 (1985) 311–315.
[43] B. Gurung, L. Yu, C.A. Yu, Stigmatellin induces reduction of iron–sulfur protein in the oxidized cytochrome bc1 complex, J. Biol. Chem. 283 (2008) 28087–28094.
[44] A.R. Crofts, V.P. Shinkarev, S.A. Dikanov, R.I. Samoilova, D. Kolling, Interactions of quinone with the iron–sulfur protein of the bc(1) complex: is the mechanism spring-loaded? Biochim. Biophys. Acta 1555 (2002) 48–53.
[45] V.P. Shinkarev, D.R. Kolling, T.J. Miller, A.R. Crofts, Modulation of the midpoint potential of the [2Fe–2S] Rieske iron sulfur center by Qo occupants in the bc1 complex, Biochemistry 41 (2002) 14372–14382.
[46] E. Darrouzet, M. Valkova-Valchanova, F. Daldal, Probing the role of the Fe–S subunit hinge region during Q(o) site catalysis in *Rhodobacter capsulatus* bc(1) complex, Biochemistry 39 (2000) 15475–15483.
[47] E. Darrouzet, M. Valkova-Valchanova, F. Daldal, The [2Fe–2S] cluster E(m) as an indicator of the iron–sulfur subunit position in the ubihydroquinone oxidation site of the cytochrome bc1 complex, J. Biol. Chem. 277 (2002) 3464–3470.
[48] E. Darrouzet, F. Daldal, Movement of the iron–sulfur subunit beyond the ef loop of cytochrome b is required for multiple turnovers of the bc1 complex but not for single turnover Qo site catalysis, J. Biol. Chem. 277 (2002) 3471–3476.
[49] E. Darrouzet, F. Daldal, Protein-protein interactions between cytochrome b and the Fe–S protein subunits during QH2 oxidation and large-scale domain movement in the bc1 complex, Biochemistry 42 (2003) 1499–1507.
[50] H. Tian, L. Yu, M.W. Mather, C.A. Yu, Flexibility of the neck region of the Rieske iron–sulfur protein is functionally important in the cytochrome bc1 complex, J. Biol. Chem. 273 (1998) 27953–27959.
[51] V.H. Obungu, Y. Wang, S.M. Amyot, C.B. Gocke, D.S. Beattie, Mutations in the tether region of the iron–sulfur protein affect the activity and assembly of the cytochrome bc(1) complex of yeast mitochondria, Biochim. Biophys. Acta 1457 (2000) 36–44.
[52] M. Brugna, S. Rodgers, A. Schricker, G. Montoya, M. Kazmeier, W. Nitschke, I. Sinning, A spectroscopic method for observing the domain movement of the Rieske iron–sulfur protein, Proc. Natl. Acad. Sci. U. S. A. 97 (2000) 2069–2074.
[53] E.A. Berry, M. Guergova-Kuras, L.S. Huang, A.R. Crofts, Structure and function of cytochrome bc complexes, Annu. Rev. Biochem. 69 (2000) 1005–1075.
[54] E.A. Berry, L.S. Huang, Observations concerning the quinol oxidation site of the cytochrome bc1 complex, FEBS Lett. 555 (2003) 13–20.
[55] E.A. Berry, D.-W. Lee, L.-S. Huang, F. Daldal, Structural and mutational studies of the cytochrome bc1 complexes, in: N.C. Hunter, F. Daldal, M.C. Thurnauer, T.J. Beatty (Eds.), The Purple Photosynthetic Bacteria, Springer Science, 2008, pp. 425–450.
[56] R.C. Sadoski, G. Engstrom, H. Tian, L. Zhang, C.A. Yu, L. Yu, B. Durham, F. Millett, Use of a photoactivated ruthenium dimer complex to measure electron transfer between the Rieske iron–sulfur protein and cytochrome c(1) in the cytochrome bc(1) complex, Biochemistry 39 (2000) 4231–4236.
[57] A.R. Crofts, M. Guergova-Kuras, R. Kuras, N. Ugulava, J. Li, S. Hong, Proton-coupled electron transfer at the Q(o) site: what type of mechanism can account for the high activation barrier? Biochim. Biophys. Acta 1459 (2000) 456–466.
[58] P.R. Rich, The quinone chemistry of bc complexes, Biochim. Biophys. Acta 1658 (2004) 165–171.
[59] J.W. Cooley, A.G. Roberts, M.K. Bowman, D.M. Kramer, F. Daldal, The raised midpoint potential of the [2Fe2S] cluster of cytochrome bc1 is mediated by both the Qo site occupants and the head domain position of the Fe–S protein subunit, Biochemistry 43 (2004) 2217–2227.

[60] D.W. Lee, N. Selamoglu, P. Lanciano, J.W. Cooley, I. Forquer, D.M. Kramer, F. Daldal, Loss of a conserved tyrosine residue of cytochrome b induces reactive oxygen species production by cytochrome bc1, J. Biol. Chem. 286 (2011) 18139–18148.
[61] C.A. Yu, J.Z. Xia, A.M. Kachurin, L. Yu, D. Xia, H. Kim, J. Deisenhofer, Crystallization and preliminary structure of beef heart mitochondrial cytochrome-bc1 complex, Biochim. Biophys. Acta 1275 (1996) 47–53.
[62] X. Gao, X. Wen, L. Esser, B. Quinn, L. Yu, C.A. Yu, D. Xia, Structural basis for the quinone reduction in the bc(1) complex: a comparative analysis of crystal structures of mitochondrial cytochrome bc(1) with bound substrate and inhibitors at the Q(i) site, Biochemistry 42 (2003) 9067–9080.
[63] A.S. Saribas, H. Ding, P.L. Dutton, F. Daldal, Tyrosine 147 of cytochrome b is required for efficient electron transfer at the ubihydroquinone oxidase site (Qo) of the cytochrome bc1 complex, Biochemistry 34 (1995) 16004–16012.
[64] T. Wenz, R. Covian, P. Hellwig, F. Macmillan, B. Meunier, B.L. Trumpower, C. Hunte, Mutational analysis of cytochrome b at the ubiquinol oxidation site of yeast complex III, J. Biol. Chem. 282 (2007) 3977–3988.
[65] H. Palsdottir, C.G. Lojero, B.L. Trumpower, C. Hunte, Structure of the yeast cytochrome bc1 complex with a hydroxyquinone anion Qo site inhibitor bound, J. Biol. Chem. 278 (2003) 31303–31311.
[66] D. Pal, P. Chakrabarti, Cis peptide bonds in proteins: residues involved, their conformations, interactions and locations, J. Mol. Biol. 294 (1999) 271–288.
[67] J.S. Richardson, D.C. Richardson, Amino acid preferences for specific locations at the ends of alpha helices, Science 240 (1988) 1648–1652.
[68] W. Kabsch, C. Sander, Biopolymers 22 (1983) 2577–2637.
[69] E.A. Berry, Z. Zhang, H.D. Bellamy, L. Huang, Crystallographic location of two Zn(2+)-binding sites in the avian cytochrome bc(1) complex, Biochim. Biophys. Acta 1459 (2000) 440–448.
[70] K. Deng, L. Zhang, A.M. Kachurin, L. Yu, D. Xia, H. Kim, J. Deisenhofer, C.A. Yu, Activation of a matrix processing peptidase from the crystalline cytochrome bc1 complex of bovine heart mitochondria, J. Biol. Chem. 273 (1998) 20752–20757.
[71] K. Deng, S.K. Shenoy, S.C. Tso, L. Yu, C.A. Yu, Reconstitution of mitochondrial processing peptidase from the core proteins (subunits I and II) of bovine heart mitochondrial cytochrome bc(1) complex, J. Biol. Chem. 276 (2001) 6499–6505.
[72] S. Hovmoller, K. Leonard, H. Weiss, Membrane crystals of a subunit complex of mitochondrial cytochrome reductase containing the cytochromes b and c1, FEBS Lett. 123 (1981) 118–122.
[73] H. Weiss, K. Leonard, Structure and function of mitochondrial ubiquinol: cytochrome c reductase and NADH:ubiquinone reductase, Chem. Scr. 27B (1987) 73–81.
[74] J.P. di Rago, F. Sohm, C. Boccia, G. Dujardin, B.L. Trumpower, P.P. Slonimski, A point mutation in the mitochondrial cytochrome b gene obviates the requirement for the nuclear encoded core protein 2 subunit in the cytochrome bc1 complex in *Saccharomyces cerevisiae*, J. Biol. Chem. 272 (1997) 4699–4704.
[75] U. Brandt, L. Yu, C.A. Yu, B.L. Trumpower, The mitochondrial targeting presequence of the Rieske iron–sulfur protein is processed in a single step after insertion into the cytochrome bc1 complex in mammals and retained as a subunit in the complex, J. Biol. Chem. 268 (1993) 8387–8390.
[76] L.A. Graham, U. Brandt, B.L. Trumpower, Protease maturation of the Rieske iron–sulphur protein after its insertion into the mitochondrial cytochrome bc1 complex of *Saccharomyces cerevisiae*, Biochem. Soc. Trans. 22 (1994) 188–191.
[77] J.D. Phillips, L.A. Graham, B.L. Trumpower, Subunit 9 of the *Saccharomyces cerevisiae* cytochrome bc1 complex is required for insertion of EPR-detectable iron–sulfur cluster into the Rieske iron–sulfur protein, J. Biol. Chem. 268 (1993) 11727–11736.
[78] A.B. Taylor, B.S. Smith, S. Kitada, K. Kojima, H. Miyaura, Z. Otwinowski, A. Ito, J. Deisenhofer, Crystal structures of mitochondrial processing peptidase reveal the mode for specific cleavage of import signal sequences, Structure 9 (2001) 615–625.
[79] B.L. Trumpower, C.A. Edwards, Purification of a reconstitutively active iron–sulfur protein (oxidation factor) from succinate. Cytochrome c reductase complex of bovine heart mitochondria, J. Biol. Chem. 254 (1979) 8697–8706.
[80] W.D. Engel, C. Michalski, G. von Jagow, Reconstitution of the ubiquinol: cytochrome c reductase from a bc1 subcomplex and the 'Rieske' iron–sulfur protein isolated by a new method, Eur. J. Biochem. 132 (1983) 395–407.
[81] Y. Shimomura, M. Nishikimi, T. Ozawa, Isolation and reconstitution of the iron–sulfur protein in ubiquinol–cytochrome c oxidoreductase complex. Phospholipids are essential for the integration of the iron–sulfur protein in the complex, J. Biol. Chem. 259 (1984) 14059–14063.
[82] D. Gonzalez-Halphen, M. Vazquez-Acevedo, B. Garcia-Ponce, On the interaction of mitochondrial complex III with the Rieske iron–sulfur protein (subunit V), J. Biol. Chem. 266 (1991) 3870–3876.
[83] M. Valkova-Valchanova, E. Darrouzet, C.R. Moomaw, C.A. Slaughter, F. Daldal, Proteolytic cleavage of the Fe–S subunit hinge region of *Rhodobacter capsulatus* bc(1) complex: effects of inhibitors and mutations, Biochemistry 39 (2000) 15484–15492.
[84] R.S. Ramabadran, D.S. Beattie, Processing of the intermediate form of the iron–sulfur protein of the BC1 complex to the mature form after import into yeast mitochondria, Arch. Biochem. Biophys. 296 (1992) 279–285.
[85] J.H. Nett, B.L. Trumpower, Intermediate length Rieske iron–sulfur protein is present and functionally active in the cytochrome bc1 complex of *Saccharomyces cerevisiae*, J. Biol. Chem. 274 (1999) 9253–9257.
[86] R.J. Morris, A. Perrakis, V.S. Lamzin, ARP/wARP and automatic interpretation of protein electron density maps, Methods Enzymol. 374 (2003) 229–244.
[87] H. Senn, F. Guerlesquin, M. Bruschi, K. Wuthrich, Coordination of the heme iron in the low-potential cytochromes c-553 from Desulfovibrio vulgaris and *Desulfovibrio desulfuricans*. Different chirality of the axially bound methionine in the oxidized and reduced states, Biochim. Biophys. Acta 748 (1983) 194–204.
[88] T.A. Jones, J.-Y. Zhou, S.W. Cowan, M. Kjeldgaard, Improved methods for building protein models in electron density maps and the location of errors on these models, Acta Crystallogr. A47 (1991) 110–119.
[89] P.J. Kraulis, MOLSCRIPT: a program to produce both detailed and schematic plots of protein structures, J. Appl. Crystallogr. 24 (1991) 946–950.
[90] E.A. Merritt, M.E. Murphy, Raster3D Version 2.0. A program for photorealistic molecular graphics, Acta Crystallogr. D Biol. Crystallogr. 50 (1994) 869–873.
[91] C. Combet, C. Blanchet, C. Geourjon, G. Deleage, NPS@: network protein sequence analysis, Trends Biochem. Sci. 25 (2000) 147–150.